



Article

Synthesis of Thiol Derivatives of Biological Active Compounds for Nanotechnology Application

Katarzyna Sidoryk ^{1,*}, Olga Michalak ¹, Marek Kubiszewski ², Andrzej Leś ³,
Marcin Cybulski ¹, Elżbieta U. Stolarczyk ² and Jan Doubsky ⁴

¹ Department of Biomedical Technology, Cosmetic Chemicals and Electrochemistry, Team of Chemistry, Łukasiewicz Research Network—Industrial Chemistry Institute, 8 Rydygiera Str., 01-793 Warsaw, Poland; o.michalak@ifarm.eu (O.M.); m.cybulski@ifarm.eu (M.C.)

² Analytical Department, Łukasiewicz Research Network—Industrial Chemistry Institute, 8 Rydygiera Str., 01-793 Warsaw, Poland; m.kubiszewski@ifarm.eu (M.K.); e.stolarczyk@ifarm.eu (E.U.S.)

³ Faculty of Chemistry, University of Warsaw, 1 Pasteur Str., 02-093 Warsaw, Poland; ales@tiger.chem.uw.edu.pl

⁴ Zentiva k.s., U Kabelovny 130, 102 37 Prague 10, Czech Republic; Jan.Doubsky@zentiva.com

* Correspondence: k.sidoryk@ifarm.eu

Academic Editor: Derek J. McPhee

Received: 14 July 2020; Accepted: 30 July 2020; Published: 30 July 2020



Abstract: An efficient method of thiol group introduction to the structure of common natural products and synthetic active compounds with recognized biological efficacy such genistein (1), 5,11-dimethyl-5H-indolo[2,3-b]quinolin (2), capecitabine (3), diosgenin (4), tigogenin (5), flumetasone (6), fluticasone propionate (7), ursolic acid methyl ester (8), and β -sitosterol (9) was developed. In most cases, the desired compounds were obtained easily via two-step processes involving esterification reaction employing S-trityl protected thioacetic acid and the corresponding hydroxy-derivative, followed by removal of the trityl-protecting group to obtain the final compounds. The results of our preliminary experiments forced us to change the strategy in the case of genistein (1), and the derivatization of diosgenin (4), tigogenin (5), and capecitabine (3) resulted in obtaining different compounds from those designed. Nevertheless, in all above cases we were able to obtain thiol-containing derivatives of selected biological active compounds. Moreover, a modelling study for the two-step thiolation of genistein and some of its derivatives was accomplished using the density functional theory (B3LP). A hypothesis on a possible reason for the unsuccessful deprotection of the thiolated genistein is also presented based on the semiempirical (PM7) calculations. The developed methodology gives access to new sulphur derivatives, which might find a potential therapeutic benefit.

Keywords: thiol derivatives; synthetic methodology; theoretical studies; nanoparticles; biological active compounds

1. Introduction

The sulfur atoms are important structural motifs presented in a number of biologically active natural β -lactam-antibiotics such as penicillin and fusaperazine as well as synthetic drugs, like amoxicillin, cefoxitin, and thienamicin for treatment in bacterial infections [1]. Moreover, sulfur-containing compounds have been utilized as excellent ligands for bounding to metal nanoparticles, especially to Au-nanoparticles, because of a very strong interaction of sulfur nucleophiles with gold nanoparticles [2,3], and gold surface monolayers [4]. The use of the thiol groups to link biologically active compounds to gold nanoparticles is well known and established [5,6]. It is known, that such conjugates may improve therapeutic efficacy of many drugs by: (i) transporting the drug directly to the target/receptor, (ii) increasing solubility in water, (iii) stability, (iv) bioavailability, and

(v) by increasing the cell membrane permeability [7]. Furthermore, the gold nanoparticles coated through a terminal sulfur atom with selected proteins have already found an application in studies of organogenesis [8] and also in clinical diagnostics [9].

Therefore, the synthesis of thiol-containing compounds is a very important field of interest, but still a challenging one, because of the known sensitivity of thiol-groups towards oxidation (resulting in disulfide bond formation) and a relatively high reactivity of thiol-groups towards alkylating and/or acylating reagents [10]. In the present study, an efficient method of thiol-group introduction to the structure of common natural products and synthetic active compounds with recognized biological efficacy such as: genistein (1), 5,11-dimethyl-5*H*-indolo[2,3-*b*]quinolin (2), capecitabine (3), diosgenin (4), tigogenin (5), flumethasone (6), fluticasone propionate (7), ursolic acid methyl ester (8), and β -sitosterol (9) was developed (Figure 1). According to the literature, compounds 1–9 and their respective derivatives show anticancer [11–13], antibacterial [14], antifungal [15], and anti-inflammatory [13,15,16] activities. Some of them are widely used in therapy as the registered drugs: flumethasone [17], fluticasone propionate [18], and capecitabine [19,20].

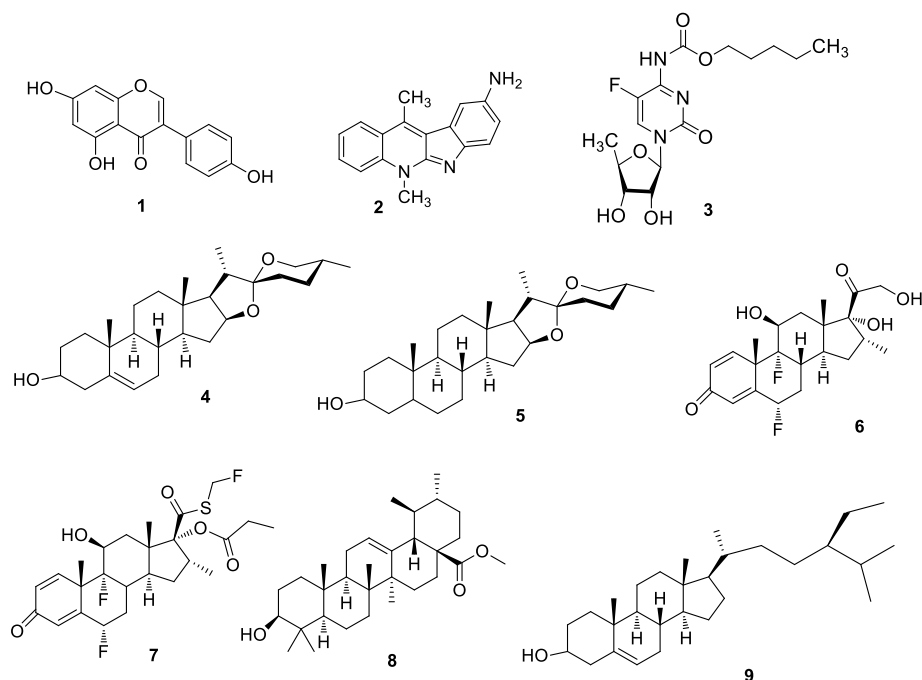


Figure 1. Structures of active compounds: 1—genistein, 2—9-amino-5,11-dimethyl-5*H*-indolo[2,3-*b*]quinoline, 3—capecitabine, 4—diosgenin, 5—tigogenin, 6—flumethasone, 7—fluticasone propionate, 8—ursolic acid methyl ester, 9— β -sitosterol.

Genistein which is one of the best investigated natural compounds, which deserves special attention. It shows potent anticancer activity but poor bioavailability, which the latest studies confirm [21,22]. Moreover, this isoflavone, which was isolated in 1899 from a flowering plant *Genista tinctoria*, exhibits other important activities, such as antiangiogenic, antioxidant, and anti-inflammatory activities. Unfortunately, despite interesting biological properties, the clinical application of genistein is still limited mainly because of its low solubility in water [23].

A similar problem occurs with 5,11-dimethyl-5*H*-indolo[2,3-*b*]quinoline, which also is a natural compound. Many derivatives of 5,11-dimethyl-5*H*-indolo[2,3-*b*]quinoline were synthesized for improving its therapeutic effect. The best results were achieved when selected amino acids or peptides were linked to an indolo[2,3-*b*]quinoline core. In vitro and in vivo studies proved that these new conjugates exhibit a higher anticancer activity against A549, MCF-7, and LoVo cells compared to

unsubstituted indolo[2,3-b]quinolone [12], but the problem of the low bioavailability has not been resolved so far.

Collectively, the bioavailability and biological activity of genistein, 5,11-dimethyl-5*H*-indolo[2,3-b]quinoline, and all above compounds (Figure 1) can be improved by chemical modification of their structures as well as creating nanoparticles with gold nanoparticles (AuNPs). Our initial study indicated that genistein conjugated with AuNPs achieved higher levels of cytotoxicity compared with free genistein [24]. This encourages us to intensify studies on AuNPs-Genistein as a candidate enhancing the anticancer effect of genistein. Unfortunately, the physical interaction of most of the drugs with the surface of the gold nanoparticle [24–26] is typically rather weak and unstable. Consequently, drugs on the nanoparticle may be replaced by other compounds that interact much more strongly with the nanoparticle surface. This can also lead to the aggregation of nanoparticles. Therefore, we focused on the synthesis of biological active compounds modified by a thiol-bearing linker as new derivatives.

The compounds 1–9 mentioned above were selected for our studies with respect to important criteria; first of all, their known biological activities. Secondly, some of them have unsatisfactory properties limiting their use as drugs, i.e., bioavailability [23], water solubility [27], and high toxicity which eventually limit their therapeutic window [28]. These parameters could be improved by incorporation of a thiol linker into their structures, which might also serve an opportunity for the future synthesis of gold nanoparticles (AuNPs) via S-Au covalent bonds. These gold nanoparticle-based drug delivery systems may overcome the limitations related to toxicity [29] and enhance the bioactivity of drugs as well [30].

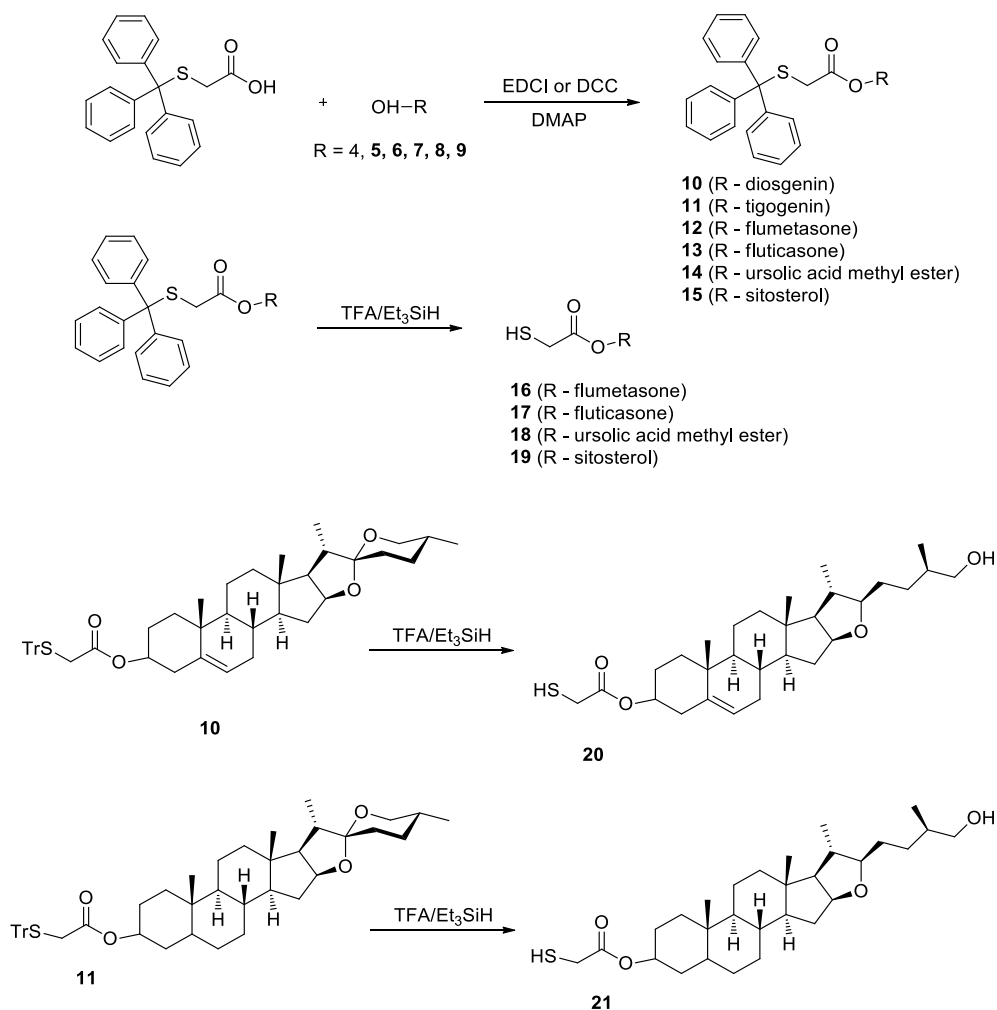
In present work we focused on developing a methodology to attach a thiomethylcarbonyl linker via ester or amide bonds in order to synthesize the thiol-containing derivatives of compounds 1–9 as promising substrates for a AuNPs-based drug delivery system. In most cases, the expected products were obtained easily by a two-step process involving esterification reaction of trityl-protected 2-thioacetic acid, followed by the removal of the protecting group to obtain the final compounds. The results of our preliminary experiments forced us to change this strategy for genistein (1) and the derivatization of diosgenin (4), tigogenin (5), and capecitabine (3). In these cases, unexpected products, different from the designed ones, were obtained to our surprise. Nevertheless, in all cases, we were able to obtain new thiol-containing derivatives of the selected biologically active compounds.

2. Results and Discussion

2.1. Chemistry

The synthesis of thiol derivatives of compounds 4, 5, 6, 7, 8, and 9 is presented in Scheme 1. The coupling of diosgenin (4), tigogenin (5), flumethasone (6), fluticasone propionate (7), ursolic acid methyl ester (8), and β -sitosterol (9) with the 2-(tritylthio)acetic acid, in the presence of DCC (*N,N'*-dicyclohexylcarbodiimide) or EDCI (*N*-ethyl-*N'*-(3-dimethylaminopropyl)carbodiimide hydrochloride) was performed according to our previously described method [4]. The esterification afforded the desired products in high yields (70 to 98 %). The only exception represents tigogenin (5) where the esterification provided the product in moderate yield of 54 %. The crude products were purified by column chromatography on silica gel to obtain the products 10–15 as white solids or foams. The deprotection of compounds 10–15 was performed using a TFA (trifluoroacetic acid)/Et₃SiH (triethylsilane) system at 0 °C under nitrogen atmosphere within 30–60 min (thin layer chromatography (TLC) monitoring), followed by triethylamine quenching. The final products 16–21 (Scheme 1, Figure 2) were obtained with moderate to high yield in a range of 51 to 93%. As it was confirmed by 1D and 2D NMR experiments for 20 and 21 compounds, trityl-group removal under mild acidic condition at room temperature resulted in additional spiroketal ring opening. Our results were consistent with those known from the literature [13,31,32], where diosgenin and tigogenin analogs with opened F-ring exhibited high biological activity [13,31,32]. Therefore, we decided to include these two derivatives (20 and 21) into further investigation as well. The structures of all new compounds (9–21) were

confirmed unambiguously by extended 1D and 2D NMR experiments (see Experimental Section, and Supplementary Materials) as well as HRMS.



Scheme 1. General method of the synthesis of thiol derivatives of flumetasone (**16**), fluticasone propionate (**17**), ursolic acid methyl ester (**18**), β -sitosterol (**19**), diosgenin (**20**), and tigogenin (**21**).

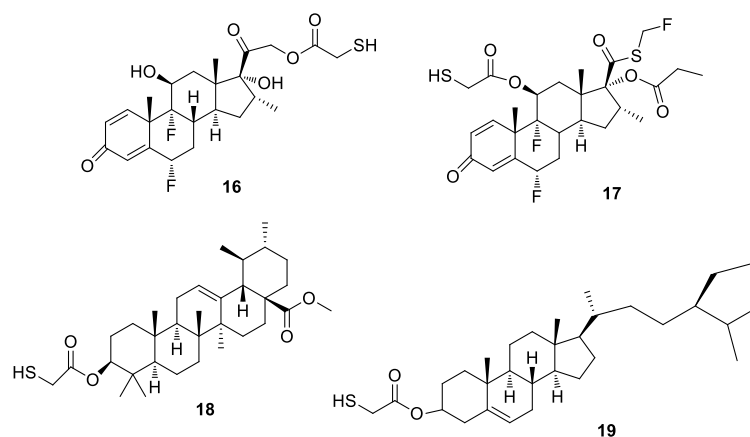
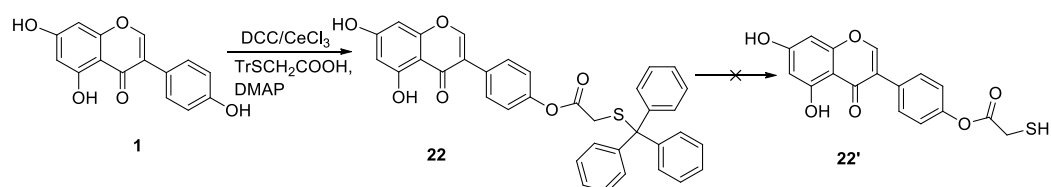


Figure 2. Structures of thiol derivatives of flumetasone (**16**), fluticasone propionate (**17**), ursolic acid methyl ester (**18**), and β -sitosterol (**19**).

Unfortunately, our efficient two-step procedure of thiol derivative preparation failed in the case of genistein (**1**) completely, and no product of 2-(tritylthio)acetic acid esterification was detected. Despite the use of higher equivalents of DCC or EDCI, the elongation of reaction time, the change of solvent (DCM (dichloromethane), THF, DMF), or the temperature increase, only the unreacted substrates were observed in the reaction mixture. Perhaps, the difficulty to directly produce genistein (**1**) ester is caused by lower nucleophilicity of the phenolic OH-groups and/or by inter- and intramolecular hydrogen bond formation (for example between 5-OH and 3-C=O). This effect may be partially neutralized by the complexation with cerium chloride which lead to the rearrangement of charge densities in substrates of esterification. Moreover, the phenolic group of genistein (**1**) is sensitive toward oxidizing agents and to bases which could negatively influence the esterification process. After a rigorous literature search, only few examples of phenolic hydroxyl groups direct esterification were found by using $\text{Me}_2\text{NSO}_2\text{Cl}$ [33], montmorillonite- Ti^{4+} [34], metal triflates [35], $\text{TiO}(\text{acac})_2$ [36], diarylammonium arensulfate [37], and tosyl chloride under solvent-free conditions [38]. Recently, the efficient new methodology of carboxylic acid esterification with phenols was described by the groups of Gilles and Hano [39,40]. The authors performed studies of juglone esterification with different fatty acids using DCC in the presence of DMAP (4-(dimethylamino)pyridine) as a condensation agents (Steglich esterification) with additional Lewis acid as a catalyst (cerium chloride CeCl_3). The Gilles research proved that the cerium chloride, a very oxophilic Lewis acid, easy to handle and with low toxicity, considerably increased the yield of esterification. This work inspired us to follow the protocol for synthesizing tritylthiol derivatives of **1**. The addition of CeCl_3 to the reaction mixture gave the expected product **22** with a moderate yield of 40% (Scheme 2). The **22** the structure was confirmed by NMR and HRMS studies. It is worth noting that according to this methodology, the ester **22** was prepared in one step. Thus, the preparation of appropriate acyl chloride from 2-(tritylthio)acetic acid and toxic reagents like SOCl_2 and pyridine was excluded from the procedure.

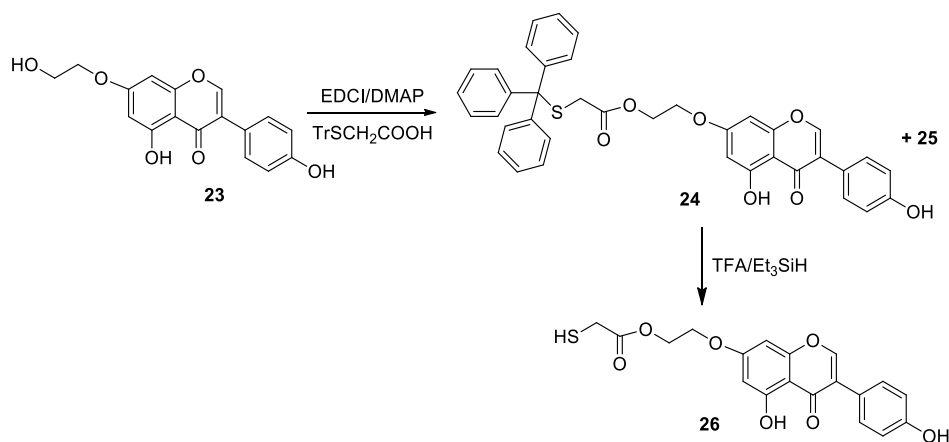


Scheme 2. Synthesis of the tritylthiol derivative of genistein (**1**).

Encouraged by the above result, we subjected the protected derivative **22** to a deprotection reaction under the same as conditions as before (TFA/ Et_3SiH). Surprisingly, we were able to detect only the starting material in the reaction mixture. Even changes of the reaction conditions (prolonged reaction time, increased temperature up to 60°C) had no influence on the reaction course. Therefore, we decided to study a new reagent system including both Lewis and protic acids according to the procedure described by the Herczegh group [41]. The detritylation of **22** was carried out using a cocktail containing boron trifluoride diethyl etherate ($\text{BF}_3 \cdot \text{Et}_2\text{O}$) as a Lewis acid, 1,1,1,3,3,3-hexafluoroisopropanol (HFIP) as a mild protic acid, and triethylsilane (Et_3SiH) as a reducing agent. Unfortunately, the treatment of **22** with this three-component cocktail led only to a decomposition of the starting material (even when the amount of $\text{BF}_3 \cdot \text{Et}_2\text{O}$ was decreased to 0.065 equiv.). We also examined another mild detritylation method using *p*-toluenesulfonic acid, but the results were unsatisfactory again.

The failure of **22** deprotection prompted us to design another thiol-derivative of genistein (**1**), i.e., compound **26** (Scheme 3). In order to achieve this goal, we synthesized the known analogue of genistein (**23**) with hydroxyethyl substituent at 7-OH according to the procedure by the Gryniewicz group [42,43]. Subsequently, **23** was transformed into the tritylthiol derivative (**24**) using our standard procedure (Scheme 3) with a yield of 80%. The traces of di-substituted **25** was also isolated from the crude material (Figure 3) and characterized by NMR technique. Consequently, the intermediate **24**, upon treatment with the mixture of TFA/ Et_3SiH , gave the desired product **26** in 80% yield. The structure

was determined by NMR and HRMS analyses. This result proved clearly that this simple experimental protocol works very effectively for the aliphatic hydroxyl group separated from the chromenone ring of genistein.



Scheme 3. Synthesis of thiol derivative of genistein.

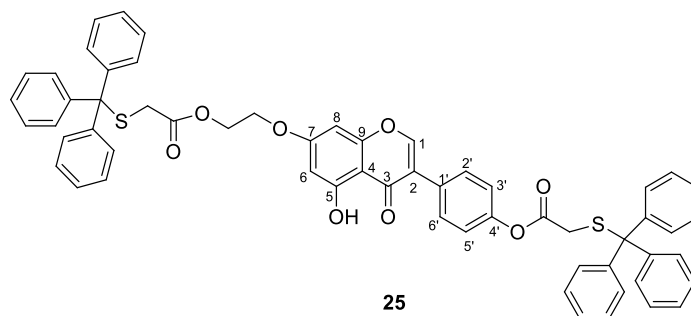
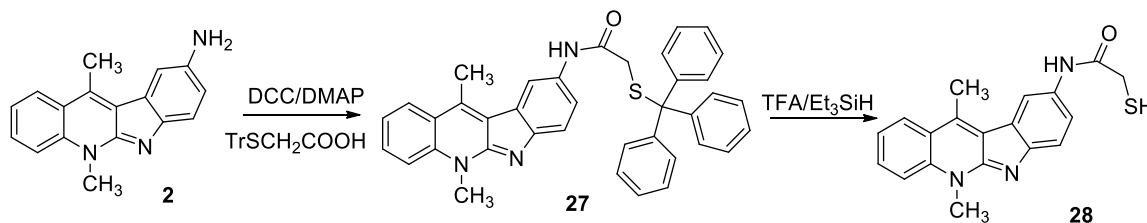


Figure 3. Structure of the impurity 25.

The syntheses of the thiol derivatives of 5,11-dimethyl-5*H*-indolo[2,3-*b*]quinoline (2) and capecitabine (3) are depicted in (Scheme 4) and (Scheme 5). In the first step of 28 synthesis, the amino group of 2 reacts with TrSCH₂COOH under standard conditions affording thus the amide 27 in 95% yield. The subsequent deprotection using a TFA/Et₃SiH system provided the product 28 in 84% yield. It should be noted that we did not observe any cleavage of the amide bond during the deprotection.

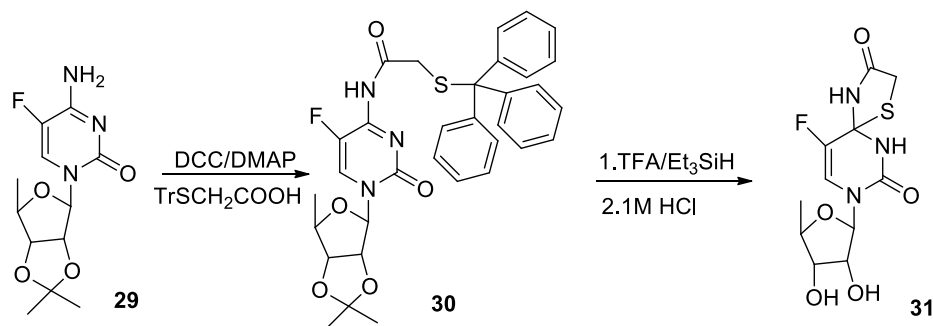


Scheme 4. Synthesis of thiol derivative of 5,11-dimethyl-5*H*-indolo[2,3-*b*]quinoline.

In an effort to obtain a thiol derivative of capecitabine (3), we utilized its known derivative 29 (Scheme 5) [19]. To our satisfaction, the acylation of 29 yielded 30 in 73% yield smoothly. The complete deprotection of trityl and isopropylidene protecting groups was achieved by a two-step protocol. In the first step, the trityl group was removed using TFA/Et₃SiH, and the thus obtained crude material (containing traces of the compound 31 already) was treated with 1M HCl to complete the isopropylidene group removal. The thus obtained product 31 was purified by column chromatography, and its structure was determined by NMR studies. It was found that the compound is a spiro-compound containing

an additional oxothiazolidine ring. This ring closure results likely from the thiol-group formed as an intermediate in addition to the tautomeric imine type bond in capecitabine derivative under the acid-catalyzed conditions. The reactions with electron-rich as well as electron-deficient aromatic *N*-acyl imines with a broad range of aliphatic and aromatic thiols are well known and were reported, e.g., by Antilla and co-workers [44], the Masuda group [45], and Zhao [46].

We believe that even compound **31** might be capable as a ligand creating metal nanoparticles with gold, platinum, or silver. Therefore, we decided to involve this derivative into our further investigation. The structures of all new compounds were confirmed by NMR as well as HRMS studies.



Scheme 5. Synthesis of thiol derivative of capecitabine.

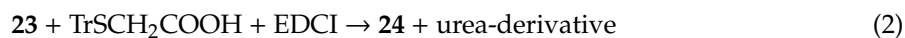
2.2. Theoretical Models of Synthesis of Thiol-Genistein Derivatives

The protection of genistein (**1**) with the tritylthiol reagent (Scheme 2) was modeled with the following equation:

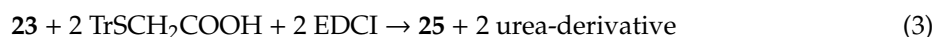


According to the calculated difference of the Gibbs free energy (details in the Table S1) of molecules composing products and substrates of this equation, the reaction energy output of about -43.0 kcal/mol was obtained, indicating a spontaneous reaction. However, in our laboratory, it was observed that the above reaction does not proceed under standard conditions. Fortunately, after addition of the CeCl_3 catalyst, this deprotection reactions afforded high yield, and this corroborates the theoretical predictions based on thermodynamic grounds. The molecular model of the role of the CeCl_3 catalyst is to be investigated. One can hypothesize that the cerium cation coordinates the reagents which are now positioned close together facilitating the reaction.

The reaction of the genistein derivative (**23**) following the Scheme 3 (top) was modeled with the equation:



The Gibbs free energy output was calculated to be about -30.8 kcal/mol. Again, this reaction was predicted to go spontaneously. In the course of the synthesis of **24**, the impurity **25** (Figure 3) was found. Both terminal hydroxyl groups in **25** are protected by tritylthiol reagent. The corresponding model reaction is given below.

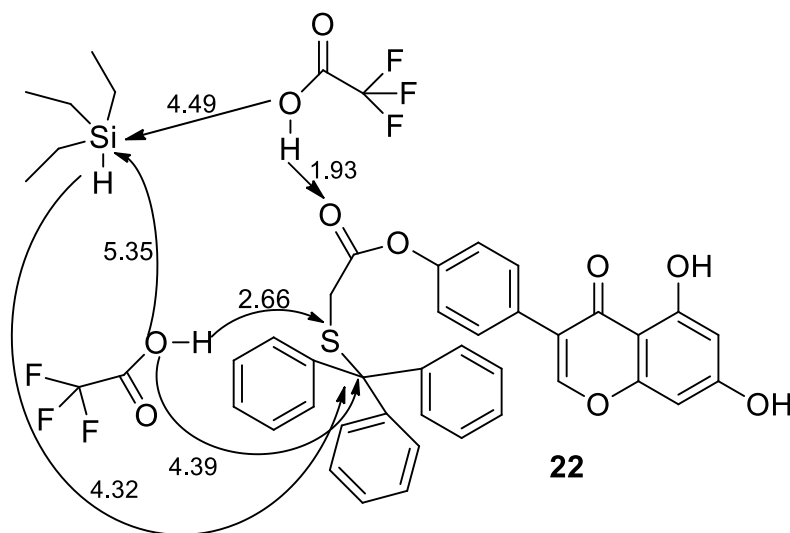


A Gibbs free energy output of about -54.6 kcal/mol was calculated, again pointing to a spontaneous reaction. Thus, the theoretically predicted spontaneous model reactions of **23** with $\text{TrSCH}_2\text{COOH}$ and EDCI corroborate laboratory observations.

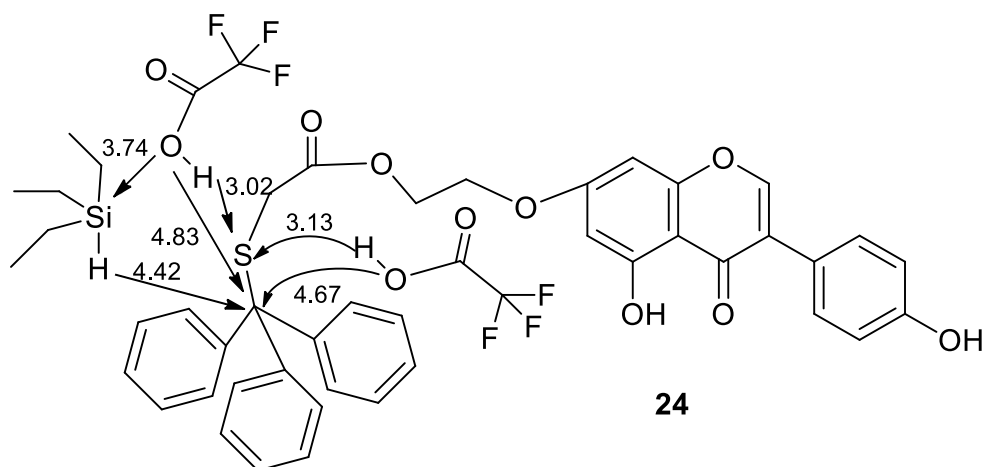
An intriguing case of deprotection failure of **22** under commonly used reagents TFA/ Et_3SiH prompted us to take a deeper look into the molecular mechanism of the reaction.

A simple look at the chemical formula of **22** and **24** suggests that the $-\text{CH}_2-\text{CH}_2-\text{O}-$ linker in **24** removes a possible sterical hindrance of the deprotection reaction. It is a problem that the phenyl group

does not interact directly with the reaction center being the Tr-S bond. An insertion of the $-\text{CH}_2\text{-CH}_2\text{-O}-$ linker in **24** has likely another role different from a simple alleviation of the phenyl ring. In a search for the molecular basis of deprotection hindrance in **22**, two mechanisms were suggested, one for a hypothetical deprotection of **22** (Scheme 6) and another one for **24** (Scheme 7). Details are given below, but we briefly summarize our idea here. We think the linker can influence on the spatial rearrangement of the TFA molecules around the reaction center. As a consequence of a TFA rearrangement in **22** different from **24**, a subsequent attack of Et_3SiH on TrTFA is blocked in **22**, but it is allowed in **24**. One can therefore say that the linker influences indirectly the deprotection reaction. Now, some quantum mechanical considerations are presented.

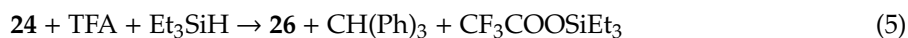
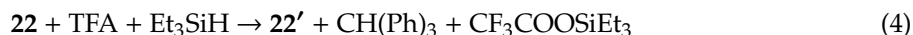


Scheme 6. Proposed mechanism of blocking the **22** deprotection. Initially, a weak C(trityl)—S bond is broken, leading to the formation of triphenylcarbenium cation which is supposed to join the TFA anion and form the TrTFA molecule. The H-bonded TFA molecule blocks the approach of a hydrophobic Et_3SiH towards the TrTFA molecule. The Et_3SiH molecule is located too far from this TrTFA molecule to complete the deprotection which arrested.



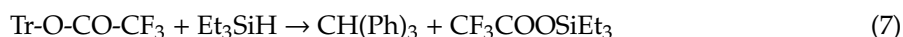
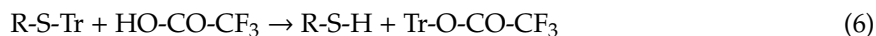
Scheme 7. Proposed mechanism of **24** deprotection. There are two TFA molecules around the Tr-S- CH_2 - residue of **24** pointing their hydrogens towards the S atom and weakening the C(trityl)-S bond. There is more freedom around the Tr-S- CH_2 - residue making possible the access of TFA anion and Et_3SiH molecules to **24** and promoting the deprotection reaction.

At first the following model reactions were considered:



Following the results of the present calculations, one can suggest that for both model reactions, the Gibbs energy out becomes nearly identical, i.e., -47.3 kcal/mol and -47.8 kcal/mol for the reaction with **22** and **24**, respectively. As long as the deprotection of **22** is not observed experimentally, one may consider the presence of a certain steric hindrance blocking the reaction.

In the search of such a steric hindrance, our attention was focused on an interesting paper of Imagawa et al. 2003 [47]. In this paper, a mechanism of triethylsilyl triflate-catalyzed reductive cleavage of trityl ether (R-O-Tr) with triethylsilane was proposed. An original idea was promoted of an equilibrium between trityl ether and triethylsilyl ether as well as a consecutive fast formation of triphenylmethane and alcohols R-OH (R being e.g., various pivaloyl or benzoyl groups). Taking into account a formal similarity of R-O-Tr and R-S-Tr structures, two model reactions were proposed in the form of (Equation (1)) and (Equation (2)):



where R denotes the **22** or **24** residues. Following the calculated Gibbs free energies of the reaction components, it was predicted that the reaction of Equation (1) becomes nearly reversible based on the Gibbs free energy output of -3.8 kcal/mol (R = **22**) and -4.3 kcal/mol (R = **24**). The reaction (Equation (2)) should be strongly shifted to the right as it can be concluded from the Gibbs free energy output of about -43.5 kcal/mol. In view of the above model reactions, one can suggest that the yet unknown steric hindrance should affect the components shown in the reaction (Equation (1)). The Gibbs free energy output of the reaction (Equation (1)) is small and likely to be sensitive to various intermolecular interactions in the reaction mixture.

Simplified 3D models of ternary complexes [**22**—TFA—Et₃SiH] and [**24**—TFA—Et₃SiH] were designed in order to find possible reaction paths leading to the products. Tentatively, it was assumed that the deprotection reaction runs according to the following steps:

Step 1: TFA approaches the thiol-residue of **22** or **24**. The COOH residue of TFA forms a H-bond with the thiol sulfur atom. It occurs a proton transfer along this H-bond towards the sulfur atom. As a result, the S-C(trityl) bond is weakened and finally becomes broken. In this way, the trityl carbocation is formed and then joined to the TFA anion. At this step, the (hypothetical) **22'** or **26** should be formed. We take into account an experimental observation that the deprotection product of **22**, i.e., **22'** is not formed. This fact will be commented on later in the text.

Step 2: Et₃SiH approaches Tr-O-CO-CF₃ from the trityl-side pointing the Si-H bond towards the trityl carbon atom. The hydrogen atom, in fact, the hydride H(−), leaves the Et₃SiH and is attached to the trityl carbocation forming trityl methane. Simultaneously, the Et₃Si(+) carbocation moves towards the O-CO-CF₃(−) anion forming Et₃Si-O-CO-CF₃.

Schemes 6 and 7 present the basis ideas of the proposed deprotection mechanism of **22** and **24**.

This hypothesis is based on three prerequisites: the C(trityl)-S bond must be weakened and then broken, the Et₃SiH should approach the C(trityl) carbocation, and the resulting Et₃Si carbocation should approach the TFA anion. The analysis of geometry of the **22**—Et₃SiH—(TFA)₄ complex, Scheme 6, reveals a rather long intermolecular distance between Et₃SiH and one of the TFA molecules supposed to create a TFA anion (5.35 Å between the Si atom and the oxygen of the carboxyl group of TFA). It is then reasonable to conclude that the expected reaction between Et₃SiH and TFA will not occur, and therefore, the deprotection reaction will be arrested. The case of the deprotection of **24** is somewhat different. In the **24**—Et₃SiH—(TFA)₄ complex the Et₃SiH and TFA intermolecular distance is considerably shorter

(3.74 Å between the Si atom and the oxygen of the carboxyl group of TFA). Moreover, the sulfur atom of the C(trityl)-S residue of **24** is H-bonded to two TFA molecules that facilitates the break of the C(trityl)-S bond.

The distances in Å correspond to the molecular complex of **22**—Et₃SiH—(TFA)₄ and **24**—Et₃SiH—(TFA)₄ optimized with the quantum mechanical semiempirical PM7 method. Details of the 3D structures are given in the Supplementary Materials.

In the deprotection reaction, four components are present: **22** or **24**, TFA, TrTFA, and Et₃SiH. It is assumed that before the reaction is initiated, three components, i.e., **22** or **24**, TFA, and Et₃SiH should meet together forming intermolecular complexes. The TrTFA component is created in the course of reaction. Molecular models of such a complexes were designed and are composed of the following six molecules:



The 3D structures were obtained with the use of the quantum mechanical semiempirical PM7 method [48] and are available in the Supplementary Material as the Figure S1.xyz and Figure S2.xyz files for the Complex 1 and Complex 2, respectively.

The four TFA molecules represent a high concentration of trifluoroacetic acid used experimentally in the course of the deprotection reaction. One can observe in Complex 1 the formation of a medium strength hydrogen bond S—H(OOCCF₃) and relatively large interatomic distance of (Et₃Si)H—(CPh₃) and Et₃Si—O(COCCF₃) of 1.93, 4.32, and 4.49 Å, respectively. In Complex 2, the corresponding interatomic distances are 3.02, 4.42, and 3.74 Å. It is remarkable that a larger interatomic distance of Si—O (4.49 Å) in Complex 1 is found when compared to Si—O (3.74 Å) in Complex 2. Perhaps it is an indication of a weaker intermolecular interaction of Et₃SiH with solvated (by TFA) **22** molecule. The product of deprotection can be also modeled, and it is presented in the files available in the Supplementary material as the Figure S3.xyz and Figure S4.xyz for the hypothetical product or disintegration of the Complex 1 and for disintegration of the Complex 2, respectively.

Both product structures are not yet optimized. They are presented here for a tentative view of how the atom rearrangement would proceed. The energy optimization of the Complex 1 or Complex 2 does not lead by itself to the deprotection products. One can conclude that when modeling the deprotection reaction, one needs to put some impulse to start atom rearrangement. Such an energetical impulse can originate from the thermal motions or intermolecular collisions of the TFA molecules surrounding **22** or **24**. More detailed studies of these motions demand not only a static approach as presented here but rather molecular dynamics including chemical reactions with the quantum chemical approach for **22** and **24** with Et₃SiH in the bath of TFA molecules. We think this is a line for the future studies.

3. Materials and Methods

3.1. General

The ¹H and ¹³C NMR spectra of all compounds were measured using Bruker AVANCE III HD spectrometer at the 500 MHz transmitter frequency for ¹H at a temperature of 298 K. The spectra were measured at a temperature of 295 K in the CDCl₃ solution relatively to the TMS signal as a ¹H and ¹³C chemical shift standard. The NMR studies were measured using the results from one- and two-dimensional NMR spectroscopy: ¹H, ¹³C, HSQC, HMBC, and COSY. The ESI-MS spectra were recorded on a PE Biosystems Mariner mass spectrometer. The progress of the reaction was monitored by thin layer chromatography (TLC) with Merck DC-Alufolien Kieselgel 60 F₂₅₄. The chemicals and solvents were purchased from Fluka Company. Column chromatography was performed on Merck silica gel 60 (230–400 mesh).

3.2. General Procedure for the Synthesis of Compounds 10–15, 24, 27, 30

Compound **2**, **4**, **5**, **6**, **7**, **8**, **9**, **23**, or **29** (1 mM) and Tr-S-CH₂-COOH (1.2 mM) were dissolved in 10 mL dichloromethane. Then DMAP (1.5 mM) was added to the solution. To the clear solution, EDCI or DCC (1.5 mM) was added portion-wise, and the reaction was stirred for 2–24 h at RT (TLC monitoring: hexane-ethyl acetate). The mixture was treated with 10 mL water. Next, the organic solution was washed with 0.1 M NaOH and brine. The organic phase was dried over anhydrous magnesium sulphate, filtered and concentrated to the crude solid. The crude products were purified by column chromatography (hexane/ethyl acetate 5:1→1:1) to give **10–15**, **24**, **27**, or **30** as white solids or foams.

3.3. General Procedure for the Synthesis of Compounds 16–21, 26, 28

The intermediates **10–15**, **24**, or **27** (1 mM) were dissolved in 10 mL dichloromethane in argon atmosphere and cooled to 0 °C (ice bath). The colorless solution was treated with 2 mL of trifluoroacetic acid, and next, triethylsilane (0.5 mL) was immediately added to the reaction mixture. The reaction was monitored by TLC (hexane:ethyl acetate 1:1 or hexane:ethyl acetate:methanol 5:3:1), and it was completed after 20 min. Then the reaction was quenched with triethylamine (1 mL), and the solution was washed with water (20 mL) and brine (20 mL). The organic phase was evaporated to the oil at room temperature. The crude oil was purified by column chromatography (hexane:ethyl acetate 1:1 or hexane:ethyl acetate:methanol 5:3:1) to afford of **16**, **17**, **18**, **19**, **20**, **21**, **26**, or **28** as white solids or foams.

diosgenin 2-(tritylmercapto)acetate (**10**): Yield 83%, m.p. 216.1 °C, ¹HNMR (500 MHz, CDCl₃): δ 7.42–7.22 (m, 15H, Ar-H), 5.35 (d, *J* = 5.0 Hz, 1H, H-6), 4.50 (m, 1H, H-3), 4.41 (m, 1H, H-16), 3.47 (m, 1H, one of H-27 protons), 3.38 (t, *J* = 11.0 Hz, 1H, one of H-27 protons), 2.92 (s, 2H, -CO-CH₂-S-), 2.25 (m, 2H, H-4), 1.99 and 1.54 (m, 2H, H-7), 1.99 and 1.28 (m, 2H, m, H-15), 1.88 (m, 1H, H-20), 1.83 and 1.09 (m, 2H, H-1), 1.78 and 1.58 (m, 2H, H-2), 1.79 (m, 1H, H-17), 1.73 and 1.18 (m, 2H, H-12), 1.69 and 1.60 (m, 2H, H-23), 1.63 and 1.46 (m, 2H, H-24), 1.63 (m, 1H, H-25), 1.60 (m, 1H, H-8), 1.49 (m, 2H, H-11), 1.11 (m, 1H, H-14), 1.01 (s, 3H, CH₃-19), 0.97 (m, 1H, H-9), 0.97 (d, *J* = 7.0 Hz, 3H, CH₃-21), 0.79 (d, 3H, CH₃-26), 0.78 (s, 3H, CH₃-18); ¹³C NMR (125 MHz, CDCl₃): δ 169.0 (CO), 144.1 (Ar-C), 139.5 (C-5), 129.5–126.8 (Ar-C), 122.5 (C-6), 109.3 (C-22), 80.8 (C-16), 75.0 (C-3), 67.1 (-C-Ph), 66.8 (C-27), 62.0 (C-17), 56.4 (C-14), 49.8 (C-9), 41.6 (C-20), 40.2 (C-13), 39.7 (C-12), 37.8 (C-4), 36.8 (C-1), 36.7 (C-10), 35.03(-CH₂-S-), 32.0 (C-7), 31.8 (C-15), 31.4 (C-23), 31.3 (C-8), 30.3 (C-25), 28.8 (C-24), 27.5 (C-2), 20.8 (C-11), 19.3 (C-19), 17.1 (C-26), 16.3 (C-18), 14.5 (C-21). HRMS (ESI) calcd. for C₄₈H₅₈O₄SNa (M+Na)⁺: 753.3954. Found: 753.3977.

tigogenin 2-(tritylmercapto)acetate (**11**): Yield 54%, m.p. 230.3 °C, ¹HNMR (500 MHz, CDCl₃): δ 7.41–7.22 (m, 15H, Ar-H), 4.59 (m, 1H, H-3), 4.39 (m, 1H, H-16), 3.46 and 3.38 (2xm, 2H, H-27), 2.91 (s, 2H, -CO-CH₂-S-), 1.95 (m, 1H, H-20), 1.76 (m, 1H, H-17), 1.53 (m, 1H, H-8), 1.62 (m, 1H, H-25), 1.12 (m, 1H, H-5), 1.12 (m, 1H, H-14), 0.65 (m, 1H, H-9), 1.97 and 1.24 (2xm, 2H, H-15), 1.74 and 1.43 (2xm, 2H, H-2), 1.69 and 0.97 (2xm, 2H, H-1), 1.66 and 0.89 (2xm, 2H, H-7), 1.52 and 1.29 (2xm, 2H, H-4), 1.69 and 1.13 (2xm, 2H, H-12), 1.67 and 1.59 (2xm, 2H, H-23), 1.62 and 1.46 (2xm, 2H, H-24), 1.48 and 1.28 (2xm, 2H, H-11), 1.26 (2xm, 2H, H-6), 0.96 (d, *J* = 10Hz, 3H, CH₃-21), 0.81 (s, 3H, CH₃-19), 0.75 (s, 3H, CH₃-18), 0.79 (d, *J* = 5Hz, 3H, CH₃-26); ¹³C NMR (125 MHz, CDCl₃): δ 169.1 (CO), 144.1 (Ar-C), 129.6–126.8 (Ar-C), 109.2 (C-22), 80.8 (C-16), 74.8 (C-3), 67.0 (-C-Ph), 66.8 (C-27), 62.1 (C-17), 56.2 (C-14), 54.1 (C-9), 44.5 (C-5), 41.6 (C-20), 40.5 (C-13), 40.0 (C-12), 36.6 (C-1), 36.1 (-CH₂-S-), 35.5 (C-10), 35.0 (C-8), 33.7 (C-4), 32.1 (C-7), 31.7 (C-15), 31.3 (C-23), 30.3 (C-25), 28.8 (C-24), 28.4 (C-6), 27.2 (C-2), 21.0 (C-11), 17.1 (CH₃-26), 16.5 (CH₃-18), 14.5 (CH₃-21), 12.2 (CH₃-19). HRMS (ESI) calcd. for C₄₈H₆₀O₄SNa (M+Na)⁺: 755.4110. Found: 755.4121.

flumetasone 2-(tritylmercapto)acetate (**12**): Yield 98%, m.p. 223.0 °C, ¹HNMR (500 MHz, CDCl₃): δ 7.41–7.22 (m, 15H, Ar-H), δ 7.14 (dd, 1H, H-1), 6.40 (bs, 1H, H-4), 6.35 (dd, *J* = 10 Hz, 1H, H-2), 5.41 and 5.31 (2xm, 1H, H-6), 4.82 and 4.72 (2xd, *J* = 30 Hz, 2H, H-22), 4.35 (m, 1H, H-11), 3.11 (m, 2H, -CH₂-S-), 3.0 (m, 1H, H-16), 2.37 and 1.65 (2xm, 2H, H-12), 2.23 and 1.71 (2xm, 2H, H-7), 2.42 (m, 1H, H-8), 2.23 (m, 1H, H-14), 1.24 and 1.17 (2xm, 2H, H-15), 1.50 (s, 3H, CH₃-19), 0.99 (s, 3H, CH₃-18), 0.90

(d, $J = 5$ Hz, 3H, H-20); ^{13}C NMR (125 MHz, CDCl_3): δ 204.1 (C-21), 185.7 (C-3), 169.8 (CO, -CO-CH₂-S-), 161.65 (d, $J = 13.7$ Hz, C-5), 151.0 (C-1), 143.9 (Ar-C) 130.0 (C-2), 129.5–126.9 (Ar-C), 121.1 (d, $J = 13.0$ Hz, C-4), 98.8 (d, $J = 177.2$ Hz, C-9), 91.00 (C-17), 86.5 (d, $J = 183.9$ Hz, C-6), 71.7 (d, $J = 38.0$ Hz, C-11), 69.2 (C-22), 48.4 (C-13), 48.1 (dd, $J_1 = 22.6$ Hz, $J_2 = 3.7$ Hz, C-10), 43.7 (C-14), 36.2 (C-12), 35.9 (C-16), 33.7 (d, $J = 19.8$ Hz, C-7), 32.7 (dd, $J_1 = 19.3$ Hz, $J_2 = 11.1$ Hz, C-8), 32.0 (C-15), 34.3 (-CH₂-S-), 22.9 (d, $J = 5.4$ Hz, CH₃-19), 16.4 (CH₃-18), 14.6 (CH₃-20); HRMS (ESI) calcd. for $\text{C}_{43}\text{H}_{44}\text{O}_6\text{F}_2\text{SNa}$ (M+Na)⁺: 749.2724. Found: 749.2747.

11-O-[2-(tritylmercapto)acetyl]-fluticasone propionate (**13**): Yield 71%, m.p. 115.1 °C; ^1H NMR (500 MHz, CDCl_3): δ 7.36–7.29 (m, 15H, Ar-H), 6.67–6.66 (dd, 1H, H-1), 6.48 (s, 1H, H-4), 6.35–6.34 (dd, 1H, H-2), 5.89–5.88 (m, 1H, -S-CH₂-F), 5.79–5.78 (m, 1H, -S-CH₂-F), 5.43–5.42 (m, 1H, H-11), 5.25–5.24 (m, 1H, H-6), 3.40 (brs, 1H, H-16), 2.99–2.98 (m, 2H, -CO-CH₂-S-), 2.37–2.36 (m, 2H, -CO-CH₂-CH₃), 2.31 (m, 1H, H-12), 2.32–2.31 (m, 1H, H-8), 2.26–2.27 (m, 1H, H-14), 2.27 (m, 1H, H-7), 1.93 (m, 1H, H-12), 1.84 (m, 1H, H-7), 1.85 (m, 1H, H-15), 1.34 (m, 1H, H-15), 1.11–0.98 (m, 12H, CH₃); ^{13}C NMR (125 MHz, CDCl_3): δ 192.8 (CO-S-CH₂-F), 184.8 (CO, C-3), 172.7 (O-CO-CH₂-CH₃), 167.2 (-O-CO-CH₂-S-Tr), 159.7 (d, $J = 14.5$ Hz, C-5), 148.6 (C-1), 143.5 (Ar-C), 130.8 (C-2), 129.4–127.1 (Ar-C), 121.4 (d, $J = 13.0$ Hz, C-4), 97.5 (d, $J = 179.5$ Hz, C-9). 95.9 (C-17), 86.1 (d, $J = 185.1$ Hz, C-6), 80.7 (d, $J = 216.8$ Hz, -S-CH₂-F), 71.9 (d, $J = 40.8$ Hz, C-11), 67.6 (-C-Ph), 47.9 (C-13), 47.1 (dd, $J_1 = 33.4$ Hz, $J_2 = 3.8$ Hz, C-10), 42.6 (C-14), 36.1 (C-16), 34.9 (-CO-CH₂-S-Tr), 33.9 (C-15), 33.4 (d, $J = 20.1$ Hz, C-7), 33.1 (dd, $J_1 = 19.2$ Hz, $J_2 = 11.4$ Hz, C-8), 32.7 (C-12), 27.5 (CO-CH₂-CH₃), 23.1 (d, $J = 5.2$ Hz, CH₃), 17.1 (CH₃), 16.2 (CH₃), 9.0 (CH₃); HRMS (ESI) calcd. for $\text{C}_{46}\text{H}_{47}\text{O}_6\text{S}_2$ (M+Na)⁺: 839.2684. Found: 839.2664.

3-O-[2-(tritylmercapto)acetyl]-ursolic acid methyl ester (**14**): Yield 84%, m.p. 219.3 °C, ^1H NMR (500 MHz, CDCl_3): δ 7.41–7.22 (m, 15H, Ar-H), 5.24 (t, 1H, $J = 5$ Hz, H-12), 4.46 (m, 1H, H-3), 3.60 (s, 3H, H-31), 2.92 (d, $J = 5$ Hz, 2H, -CH₂-S-), 2.23 (d, $J = 15$ Hz, 1H, H-18), 2.00 and 1.68 (2xm, 2H, H-16), 1.90 (m, 2H, H-11), 1.77 and 1.06 (2xm, 2H, H-15), 1.58 (m, 2H, H-2), 1.67 and 1.60 (2xm, 2H, H-22), 1.63 and 1.05 (2xm, 2H, H-1), 1.52 (m, 1H, H-9), 1.51 and 1.36 (2xm, 2H, H-6), 1.48 and 1.30 (2xm, 2H, H-21), 1.48 and 1.31 (2xm, 2H, H-7), 1.34 (m, 1H, H-19), 1.07 (s, 3H, H-27), 1.00 (m, 1H, H-20), 0.93 (s, 3H, CH₃-25), 0.94 (d, $J = 10$ Hz, 3H, CH₃-30), 0.84 (m, 3H, CH₃-23), 0.84 (m, 3H, CH₃-24), 0.85 (d, $J = 5$ Hz, 3H, CH₃-29), 0.80 (m, 1H, H-5), 0.74 (s, 3H, CH₃-26); ^{13}C NMR (125 MHz, CDCl_3): δ 178.1 (C-28), 169.4 (CO), 144.1 (Ar-C), 138.2 (C-13), 129.5–126.8 (Ar-C), 125.4 (C-12), 82.1 (C-3), 67.1 (-C-Ph) 55.2 (C-5), 52.8 (C-18), 51.4 (C-31), 48.1 (C-17), 47.4 (C-9), 41.9 (C-14), 39.5 (C-8), 39.0 (C-19), 38.8 (C-20), 38.2 (C-1), 37.8 (C-4), 36.8 (C-10), 36.6 (C-22), 35.2 (-CH₂-S-), 32.8 (C-7), 30.6 (C-21), 28.1 (C-23), 27.9 (C-15), 24.2 (C-16), 23.5 (C-27), 23.4 (C-2), 23.3 (C-11), 21.2 (CH₃-30), 18.1 (C-6), 17.0 (CH₃-29), 16.9 (CH₃-26), 16.8 (CH₃-24), 15.5 (CH₃-25). HRMS (ESI) calcd. for $\text{C}_{52}\text{H}_{66}\text{O}_4\text{SNa}$ (M+Na)⁺: 809.4580. Found: 809.4597.

β -sitosterol 2-(tritylmercapto)acetate (**15**): Yield 75%, ^1H NMR (500 MHz, CDCl_3): δ 7.43–7.23 (m, 15H, Ar-H), 5.36 (d, $J = 5.0$ Hz, 1H, H-6), 4.51 (m, 1H, H-3), 2.93 (s, 2H, -CH₂-S-), 2.25 (d, $J = 5.0$ Hz, 2H, H-4), 2.01 and 1.18 (2xm, 2H, H-12), 1.85 and 1.27 (2xm, 2H, H-16), 1.97 and 1.54 (2xm, 2H, H-7), 0.94 (m, 1H, H-9), 1.81 and 1.52 (2xm, 2H, H-2), 1.84 and 1.10 (2xm, 2H, H-1), 1.67 (m, 1H, H-25), 1.58 and 1.07 (2xm, 2H, H-15), 1.49 (m, 2H, H-11), 1.44 (m, 1H, H-8), 1.36 (m, 1H, H-20), 1.33 and 1.02 (2xm, 2H, H-22), 1.27 (m, 2H, H-28), 1.18 (m, 2H, H-23), 1.12 (m, 1H, H-17), 1.00 (m, 1H, H-14), 1.00 (s, 3H, CH₃-19), 0.94 (m, 1H, H-24), 0.93 (d, $J = 5$ Hz, 3H, CH₃-21), 0.85 (m, 3H, CH₃-29), 0.85 (m, 3H, H-27), 0.82 (m, 3H, CH₃-26), 0.68 (s, 3H, CH₃-18); ^{13}C NMR (125 MHz, CDCl_3): δ 169.0 (CO), 139.5 (C-5), 144.1 (Ar-C), 129.6–126.9 (Ar-C), 122.8 (C-6), 75.1 (C-3), 67.1 (-C-Ph), 56.7 (C-14), 56.0 (C-17), 50.0 (C-9), 45.8 (C-24), 42.3 (C-13), 39.7 (C-12), 37.9 (C-4), 36.9 (C-1), 36.5 (C-10), 36.2 (C-20), 35.1 (-CH₂-S-), 33.9 (C-22), 31.9 (C-7), 31.8 (C-8), 29.1 (C-25), 28.3 (C-16), 27.6 (C-2), 26.0 (C-23), 24.3 (C-15), 23.1 (C-28), 21.0 (C-11), 19.8 (CH₃-27), 19.3 (CH₃-19), 19.0 (CH₃-26), 18.8 (CH₃-21), 12.0 (CH₃-29), 11.9 (CH₃-18). HRMS (ESI) calcd. for $\text{C}_{50}\text{H}_{66}\text{O}_2\text{SNa}$ (M+Na)⁺: 753.4681. Found: 753.4700.

flumethasone 2-mercaptoacetate (**16**): Yield 71%, m.p. 244.2 °C, ^1H NMR (500 MHz, CDCl_3): δ 7.11 (d, $J = 5$ Hz, 1H, H-1), 6.42 (s, 1H, H-4), 6.37 (dd, $J = 10$ Hz, 1H, H-2), 5.43 and 5.33 (2xm, 1H, H-6), 4.98 and 4.91 (2xd, $J = 20$ Hz, 2H, H-22), 4.40 (m, 1H, H-11), 3.42 (m, 2H, -CH₂-SH), 3.13 (m, 1H, H-16), 2.45 and 1.68 (2xm, 2H, H-12), 2.25 and 1.74 (2xm, 2H, H-7), 2.44 (m, 1H, H-8), 2.26 (m, 1H, H-14), 1.80

and 1.17 (2xm, 2H, H-15), 1.52 (s, 3H, CH₃-19), 1.04 (s, 3H, CH₃-18), 0.93 (d, *J* = 5 Hz, 3H, H-20); ¹³C NMR (125 MHz, CDCl₃): δ 204.1 (C-21), 185.5 (C-3), 170.9 (CO, -CO-CH₂-SH), 161 (C-5), 150.4 (C-1), 130.3 (C-2), 121.2 (d, *J* = 13.1 Hz, C-4), 98.7 (C-9), 90.9 (C-17), 86.5 (d, *J* = 184.2 Hz, C-6), 71.8 (d, *J* = 38.3 Hz, C-11), 69.3 (C-22), 48.5 (C-13), 48 (C-10), 43.7 (C-14), 36.5 (C-12), 35.9 (C-16), 33.7 (d, *J* = 19.8 Hz, C-7), 33.7 (C-8), 32.0 (C-15), 26.2 (-CH₂-SH), 23.0 (d, *J* = 6.0 Hz, CH₃-19), 16.5 (CH₃-18), 14.5 (CH₃-20); HRMS (ESI) calcd. for C₂₄H₃₀O₆F₂SNa (M+Na)⁺: 507.1629. Found: 507.1650.

11-O-[2-(mercapto)acetyl]-fluticasone propionate (**17**): Yield 93%, m.p. 169–170 °C; ¹H NMR (500 MHz, CDCl₃): δ 6.90–6.88 (m, 1H, H-1), 6.33–6.31 (m, 1H, H-2), 6.14 (bs, 1H, H-4), 5.93–5.91 (m, 1H, -S-CH₂-F), 5.83–5.81 (m, 1H, -S-CH₂-F), 5.67–5.58 (m, 1H, H-6), 5.24–5.23 (m, 1H, H-11), 3.88–3.87 (m, 2H, -CH₂-SH), 3.29 (s, 1H, H-16), 2.65–2.64 (m, 1H, H-8), 2.38–2.36 (m, 2H, -CO-CH₂-CH₃), 2.28 (m, 1H, H-7), 2.21 (m, 1H, H-12), 2.15–2.13 (m, 1H, H-14), 1.95 (m, 1H, H-12), 1.88 (m, 1H, H-15), 1.53 (m, 1H, H-7), 1.29 (m, 1H, H-15), 1.11–0.98 (m, 12H, CH₃); ¹³C NMR (125 MHz, CDCl₃): δ 193.1 (CO, -CO-S-CH₂-F), 183.9 (CO, C-3), 172.3 (CO, -CO-CH₂-CH₃), 167.7 (CO, -CO-CH₂-SH), 161.6 (d, *J* = 13.8 Hz, C-5), 149.9 (C-1), 129.7 (C-2), 119.7 (d, *J* = 12.5 Hz, C-4), 98.4 (d, *J* = 176.8 Hz, C-9), 95.5 (C-17), 86.4 (d, *J* = 180.8 Hz, C-6), 80.9 (d, *J* = 212.5 Hz-S-CH₂-F), 72.05 (d, *J* = 41.3 Hz, C-11), 47.6 (C-13), 47.2 (dd, *J*₁ = 22.1 Hz, *J*₂ = 3.2 Hz, C-10), 42.3 (C-14), 40.5 (-CH₂-SH), 35.7 (C-16), 33.4 (d, *J* = 19.2 Hz, C-7), 33.1 (C-15), 32.3 (C-8), 31.9 (C-12), 26.8 (-CH₂-CH₃), 22.3 (d, *J* = 5.2 Hz, CH₃), 16.7 (CH₃), 15.7 (CH₃), 8.9 (CH₃). HRMS (ESI) calcd. for C₂₇H₃₃O₆F₃S₂Na (M+Na)⁺: 597.6762. Found: 597.6758.

3-O-[2-(mercapto)acetyl]-ursolic acid methyl ester (**18**): Yield 95%, m.p. 155.8 °C, ¹H NMR (500 MHz, CDCl₃): δ 5.24 (t, *J* = 5 Hz, 1H, H-12), 4.53 (m, 1H, H-3), 3.60 (s, 3H, H-31), 3.25 (d, *J* = 5 Hz, 2H, -CH₂-SH), 2.23 (d, *J* = 15 Hz, 1H, H-18), 1.99 and 1.65 (2xm, 2H, H-16), 1.90 (m, 2H, H-11), 1.77 and 1.06 (2xm, 2H, H-15), 1.65 (m, 2H, H-2), 1.65 and 1.58 (2xm, 2H, H-22), 1.65 and 1.07 (2xm, 2H, H-1), 1.52 (m, 1H, H-9), 1.50 and 1.36 (2xm, 2H, H-6), 1.48 and 1.29 (2xm, 2H, H-21), 1.48 and 1.32 (2xm, 2H, H-7), 1.33 (m, 1H, H-19), 1.07 (s, 3H, H-27), 1.00 (m, 1H, H-20), 0.94 (s, 3H, CH₃-25), 0.94 (d, *J* = 5 Hz, 3H, CH₃-30), 0.89 (s, 3H, CH₃-23), 0.87 (m, 3H, CH₃-24), 0.86 (d, *J* = 5 Hz, 3H, CH₃-29), 0.82 (m, 1H, H-5), 0.74 (s, 3H, CH₃-26); ¹³C NMR (125 MHz, CDCl₃): δ 178.1 (C-28), 170.7 (CO), 138.2 (C-13), 125.4 (C-12), 82.4 (C-3), 55.3 (C-5), 52.8 (C-18), 51.5 (C-31), 48.0 (C-17), 47.4 (C-9), 41.9 (C-14), 39.4 (C-8), 39.0 (C-19), 38.8 (C-20), 38.2 (C-1), 37.9 (C-4), 36.8 (C-10), 36.6 (C-22), 32.8 (C-7), 30.6 (C-21), 28.0 (C-23), 27.9 (C-15), 26.9 (-CH₂-SH), 24.2 (C-16), 23.5 (C-27), 23.4 (C-2), 23.3 (C-11), 21.2 (CH₃-30), 18.1 (C-6), 17.0 (CH₃-29), 16.9 (CH₃-26), 16.7 (CH₃-24), 15.5 (CH₃-25). HRMS (ESI) calcd. for C₃₃H₅₂O₄SNa (M+Na)⁺: 567.3484. Found: 567.3475.

β-sitosterol 2-mercaptoacetate (**19**): Yield 51%, m.p. 166.7 °C, ¹H NMR (500 MHz, CDCl₃): δ 5.39 (d, *J* = 5.0 Hz, 1H, H-6), 4.64 (m, 1H, H-3), 3.22 (m, 2H, -CH₂-SH), 2.34 (m, 2H, H-4), 2.01 and 1.17 (2xm, 2H, H-12), 1.84 and 1.26 (2xm, 2H, H-16), 1.97 and 1.56 (2xm, 2H, H-7), 1.95 (m, 1H, H-9), 1.88 and 1.62 (2xm, 2H, H-2), 1.88 and 1.14 (2xm, 2H, H-1), 1.67 (m, 1H, H-25), 1.58 and 1.05 (2xm, 2H, H-15), 1.49 (m, 2H, H-11), 1.46 (m, 1H, H-8), 1.36 (m, 1H, H-20), 1.33 and 1.01 (2xm, 2H, H-22), 1.26 (m, 2H, H-28), 1.16 (2xm, 2H, H-23), 1.11 (m, 1H, H-17), 1.01 (m, 1H, H-14), 1.02 (s, 3H, CH₃-19), 0.92 (m, 1H, H-24), 0.92 (d, *J* = 5 Hz, 3H, CH₃-21), 0.84 (m, 3H, CH₃-29), 0.84 (m, 3H, H-27), 0.81 (m, 3H, CH₃-26), 0.68 (s, 3H, CH₃-18); ¹³C NMR (125 MHz, CDCl₃): δ 170.3 (CO), 139.3 (C-5), 122.9 (C-6), 75.4 (C-3), 56.6 (C-14), 56.0 (C-17), 50.0 (C-9), 45.8 (C-24), 42.3 (C-13), 39.7 (C-12), 37.9 (C-4), 36.9 (C-1), 36.5 (C-10), 36.1 (C-20), 33.9 (C-22), 31.9 (C-7), 31.8 (C-8), 29.1 (C-25), 28.2 (C-16), 27.6 (C-2), 26.9 (-CH₂-SH), 26.0 (C-23), 24.3 (C-15), 23.0 (C-28), 21.0 (C-11), 19.8 (CH₃-27), 19.3 (CH₃-19), 19.0 (CH₃-26), 18.7 (CH₃-21), 12.0 (CH₃-29), 11.8 (CH₃-18). HRMS (ESI) calcd. for C₃₁H₅₂O₂SNa (M+Na)⁺: 511.3586. Found: 511.3596.

3-O-[2-(mercapto)acetyl]-(3β, 25R)-furost-5-ene-3,26-diol (**20**): Yield 81%, m.p. 108.1 °C, ¹H NMR (500 MHz, CDCl₃): δ 5.38 (d, *J* = 5.0 Hz, 1H, H-6), 4.65 (m, 1H, H-3), 4.31 (m, 1H, H-16), 3.47 (m, 2H, H-27), 3.33 (m, 1H, H-22), 3.23 (d, *J* = 10 Hz, 2H, -CH₂-SH), 2.35 (m, 2H, H-4), 2.00 and 1.30 (2xm, 2H, H-15), 2.00 and 1.54 (2xm, 2H, H-7), 1.89 and 1.62 (2xm, 2H, H-2), 1.89 and 1.13 (2xm, 2H, H-1), 1.75 (m, 1H, H-20), 1.72 and 1.12 (2xm, 2H, H-12), 1.66 (m, 1H, H-25), 1.62 (m, 1H, H-8), 1.61 (m, 1H, H-17), 1.59 (m, 2H, H-23), 1.48 (m, 2H, H-11), 1.47 and 1.35 (2xm, 2H, H-24), 1.09 (m, 1H, H-14), 1.03 (s, 3H, CH₃-19), 1.00 (d, *J* = 5 Hz, 3H, CH₃-21), 0.95 (m, 1H, H-9), 0.91 (d, *J* = 10 Hz, 3H, CH₃-26), 0.81 (s, 3H,

CH3-18); ^{13}C NMR (125 MHz, CDCl_3): δ 170.5 (CO), 139.3 (C-5), 122.6 (C-6), 90.4 (C-22), 83.2 (C-16), 75.3 (C-3), 68.0 (C-27), 65.0 (C-17), 56.9 (C-14), 50.0 (C-9), 40.7 (C-13), 39.4 (C-12), 37.9 (C-20), 37.8 (C-4), 37.0 (C-1), 36.7 (C-10), 35.7 (C-25), 32.2 (C-15), 32.0 (C-7), 31.6 (C-8), 30.4 (C-23), 30.1 (C-24), 27.6 (C-2), 26.8 ($-\text{CH}_2\text{-SH}$), 20.6 (C-11), 19.3 (CH3-19), 18.9 (CH3-21), 16.6 (CH3-26), 16.4 (CH3-18). HRMS (ESI) calcd. for $\text{C}_{29}\text{H}_{46}\text{O}_4\text{SNa}$ (M+Na) $^+$: 513.3015. Found: 513.3035.

3-O-[2-(mercapto)acetyl]-(3 β , 25 R)-furostane-3,26-diol (**21**): Yield 54%, m.p. 122.3 $^\circ\text{C}$, ^1H NMR (500 MHz, CDCl_3): δ 4.70 (m, 1H, H-3), 4.27 (m, 1H, H-16), 3.45 (m, 2H, H-27), 3.30 (m, 1H, H-22), 3.20 (d, J = 10Hz, 2H, $-\text{CO-CH}_2\text{-S-}$), 1.98 and 1.25 (2xm, 2H, H-15), 1.82 and 1.51 (2xm, 2H, H-2), 1.73 and 1.01 (2xm, 2H, H-1), 1.73 (m, 1H, H-20), 1.67 and 1.07 (2xm, 2H, H-12), 1.66 and 0.86 (2xm, 2H, H-7), 1.65 (m, 1H, H-25), 1.60 and 1.37 (2xm, 2H, H-4), 1.58 (m, 1H, H-17), 1.57 (m, 2H, H-23), 1.51 (m, 1H, H-8), 1.48 and 1.27 (2xm, 2H, H-11), 1.45 and 1.33 (2xm, 2H, H-24), 1.26 (2xm, 2H, H-6), 1.15 (m, 1H, H-5), 1.06 (m, 1H, H-14), 0.97 (d, J = 10Hz, 3H, CH3-21), 0.89 (d, J = 5Hz, 3H, CH3-26), 0.82 (s, 3H, CH3-19), 0.76 (s, 3H, CH3-18), 0.63 (m, 1H, H-9); ^{13}C NMR (125 MHz, CDCl_3): δ 170.4 (CO), 90.2 (C-22), 83.2 (C-16), 75.1 (C-3), 67.9 (C-27), 65.1 (C-17), 56.6 (C-14), 54.1 (C-9), 44.6 (C-5), 40.8 (C-13), 40.0 (C-12), 37.9 (C-20), 36.6 (C-1), 35.7 (C-25), 35.5 (C-10), 35.2 (C-8), 33.7 (C-4), 32.1 (C-7), 32.01 (C-15), 30.3 (C-23), 30.0 (C-24), 28.4 (C-6), 27.2 (C-2), 26.8 ($-\text{CH}_2\text{-S-}$), 20.8 (C-11), 18.9 (CH3-21), 16.6 (CH3-18), 16.6 (CH3-26), 12.2 (CH3-19). HRMS (ESI) calcd. for $\text{C}_{29}\text{H}_{48}\text{O}_4\text{SNa}$ (M+Na) $^+$: 515.3171. Found: 515.3159.

4'-O-[2-(tritylmercapto)acetyl]-genistein (**22**): Compound **1** (100 mg, 0.37 mM) and Tr-S- $\text{CH}_2\text{-COOH}$ (248 mg, 0.74 mM) were dissolved in 8 mL THF. Then, DMAP (18 mg, 0.148 mM), and CeCl_3 (28 mg, 0.074 mM) were added to the solution. To the clear solution was added portionwise of DCC (382 mg, 1.85 mM), and the reaction was stirred for 24h at RT (TLC monitoring: hexane-ethyl acetate). The mixture was treated with 10 mL water, DCM (20 mL) next the organic solution was washed with 0.1 M NaOH, and brine. The organic phase dried over anhydrous magnesium sulphate, filtered and concentrated to the crude solid. The crude product was purified by column chromatography (hexane/ethyl acetate 5:1 \rightarrow 1:1) to give **22** (87 mg, 40%) as white solid. Yield 40%, m.p. 162.5 $^\circ\text{C}$; ^1H NMR (CDCl_3 , 500 MHz): δ 7.82 (s, 1H, H-1), 7.47–7.45 (m, 5H, Ar-H), 7.46–7.44 (m, 2H, H-2', H-6'), 7.29–7.21 (m, 10H, Ar-H), 7.02–7.01 (m, 2H, H-3', H-5'), 6.32 (d, 1H, H-8), 6.25 (d, 1H, H-6), 3.19 (brs, 2H, $-\text{CH}_2\text{-S-}$); ^{13}C NMR (CDCl_3 , 125 MHz): δ 180.2 (C=O), 168.1 (C=O), 164.1 (C-7), 162.1 (C-5), 158.0 (C-9), 153.1 (C-1), 150.3 (C-4'), 143.8 (C-Ar), 129.8 (C-2', C-6'), 129.4 (C-Ar), 129.3 (C-Ar), 128.5 (C-1'), 128.0 (C-Ar), 127.9 (C-Ar), 126.9 (C-Ar), 126.7 (C-Ar), 122.8 (C-2), 121.3 (C-3', C-5'), 105.2 (C-4), 99.3 (C-6), 94.1 (C-8), 67.4 ($-\text{S-C-}$), 34.6 ($-\text{CH}_2\text{-}$); HRMS (ESI) calcd. for $\text{C}_{36}\text{H}_{26}\text{O}_6\text{SNa}$ (M+H) $^+$: 609.1340. Found: 609.1348.

7-O-[2-(tritylmercaptomethylcarboxy)ethyl]-genistein (**24**): Yield 80%, m.p. 142.4 $^\circ\text{C}$; ^1H NMR (CDCl_3 , 500 MHz): δ 12.96 (s, 1H, OH-5), 9.61 (s, 1H, OH-4'), 8.40 (s, 1H, H-1), 7.38–7.37 (m, 2H, H-2', H-6'), 7.33–7.30 (m, 12H, Ar-H), 7.24–7.23 (m, 3H, Ar-H), 6.83–6.82 (m, 2H, H-3', H-5'), 6.64 (d, 1H, H-8), 6.38 (d, 1H, H-6), 4.21–4.20 (m, 4H, $-\text{CH}_2\text{-CH}_2\text{-}$), 2.99 (brs, 2H, $-\text{CH}_2\text{-}$); ^{13}C NMR (CDCl_3 , 125 MHz): δ 180.4 (C=O), 168.8 (O=C-O), 163.9 (C-7), 161.7 (C-5), 157.5 (C-4'), 157.4 (C-9), 154.4 (C-1), 143.6 (Ar-C), 130.1 (C-2', C-6'), 129.0 (Ar-C), 128.1 (Ar-C), 126.9 (Ar-C), 122.5 (C-2), 121.0 (C-1'), 115.0 (C-3', C-5'), 105.5 (C-4), 98.3 (C-6), 92.9 (C-8), 66.6 ($-\text{S-C-}$), 66.3 ($-\text{O-CH}_2\text{-CH}_2\text{-O-}$), 63.1 ($-\text{O-CH}_2\text{-CH}_2\text{-O-}$), 33.8 ($-\text{CH}_2\text{-S-}$); HRMS (ESI) calcd. for $\text{C}_{38}\text{H}_{30}\text{O}_7\text{S}$ (M+Na) $^+$: 653.1635. Found: 653.1610.

4'-O-[2-(tritylmercapto)acetyl]-7-O-[2-(tritylmercaptomethylcarboxy)ethyl]-genistein (**25**): ^1H NMR (DMSO, 500 MHz): δ 12.82 (s, 1H, OH-5), 8.52 (s, 1H, H-1), 7.59–7.57 (m, 2H, H-2', H-6'), 7.37–7.24 (m, 30H, Ar-H), 7.07–7.05 (m, 2H, H-3', H-5'), 6.68 (d, 1H, H-8), 6.41 (d, 1H, H-6), 4.22–4.21 (m, 4H, $-\text{CH}_2\text{-CH}_2\text{-}$), 3.33–3.31 (m, 2H, $-\text{CO-CH}_2\text{-}$), 2.99–2.98 (m, 2H, $-\text{CO-CH}_2\text{-}$); ^{13}C NMR (CDCl_3 , 125 MHz): δ 180.0 (C=O), 168.8 (C=O), 167.7 (C=O), 164.1 (C-7), 161.7 (C-5), 157.4 (C-9), 155.5 (C-1), 150.0 (C-4'), 143.6 (Ar-C), 130.0 (C-2', C-6'), 129.1 (Ar-C), 129.0–126.9 (Ar-C), 121.7 (C-2), 121.3 (C-3', C-5'), 105.5 (C-4), 98.5 (C-6), 93.1 (C-8), 66.9 ($-\text{S-C-Ar}$), 66.8 ($-\text{S-C-Ar}$), 66.4 ($-\text{O-CH}_2\text{-CH}_2\text{-CO}$), 63.0 ($-\text{O-CH}_2\text{-CH}_2\text{-CO}$), 34.1 ($\text{CO-CH}_2\text{-S-}$), 33.8 ($\text{CO-CH}_2\text{-S-}$); HRMS (ESI) calcd. for $\text{C}_{59}\text{H}_{46}\text{O}_8\text{S}_2$ (M+Na) $^+$: 969.2523. Found: 969.2532.

7-O-[2-(mercaptomethylcarboxy)ethyl-genistein (**26**): Yield 81 %, m.p. 168 °C; ^1H NMR (DMSO, 500 MHz): δ 12.95 (s, 1H, OH-4'), 9.61 (s, 1H, OH-5), 8.41 (s, 1H, H-1), 7.39–7.37 (m, 2H, H-2', H-6'), 6.82–6.81 (m, 2H, H-3', H-5'), 6.69–6.68 (m, 1H, H-8), 6.42–6.41 (m, 1H, H-6), 4.41–4.32 (m, 4H, -O-CH₂-CH₂-), 3.38–3.33 (m, 2H, -CH₂-SH); ^{13}C NMR (DMSO, 125 MHz): δ 180.4 (C=O), 170.8 (-O-C=O-), 163.9 (C-7), 161.7 (C-5), 157.4 (C-9), 154.4 (C-1), 130.1 (C-2'), 122.5 (C-2), 121.0 (C-1'), 115.1 (C-3'), 105.5 (C-4), 98.4 (C-6), 92.9 (C-8), 66.6 (-O-CH₂-CH₂-), 63.1 (-O-CH₂-CH₂-), 25.5 (-CH₂-SH); HRMS (ESI) calcd. for C₁₉H₁₆O₇S (M+Na)⁺: 411.0523. Found: 411.0514.

N-(5,11-dimethyl-5H-indolo[2,3-b]quinolin-9-yl)-2-(tritylmercapto)acetamid (**27**): Yield 95%, m.p. 181 °C; ^1H NMR (CDCl₃, 500 MHz): δ 8.34–8.33 (d, 1H, *J* = 5 Hz), 8.18–8.16 (dd, 1H, *J* = 5 Hz, *J* = 10 Hz), 8.01–8.00 (m, 2H), 7.75–7.70 (m, 2H), 7.59–7.57 (d, 1H, *J* = 10 Hz), 7.49–7.48 (m, 6H), 7.32–7.26 (m, 6H), 7.22–7.20 (m, 2H), 7.13–7.11 (m, 1H), 4.28 (s, 3H), 3.35 (s, 2H), 3.06 (s, 3H); ^{13}C NMR (CDCl₃, 125 MHz): δ 165.8 (C=O), 162.4, 143.8, 136.6, 130.2, 129.8, 129.4, 128.2, 127.1, 125.7, 124.5, 121.6, 121.2, 121.1, 116.1, 115.6, 114.3, 68.0, 36.7 (CH₂), 36.4, 32.9, 31.3, 15.4 (CH₃); HRMS (ESI) calcd. for C₃₈H₃₁N₃OS (M+H)⁺: 578.2248. Found: 578.2266.

N-(5,11-dimethyl-5H-indolo[2,3-b]quinolin-9-yl)-2-mercaptoacetamid (**28**): Yield 84%, m.p. 228.6 °C; ^1H NMR (CDCl₃, 500 MHz): δ 13.7 (brs, 1H), 10.37 (brs, 1H), 8.71–8.70 (m, 1H), 8.60–8.58 (d, 1H, *J* = 10 Hz), 8.33–8.31 (d, 1H, *J* = 10 Hz), 8.13–8.10 (m, 1H), 7.85–7.83 (m, 1H), 7.68–7.66 (dd, 1H, *J* = 5 Hz, *J* = 10 Hz), 7.61–7.59 (d, 1H, *J* = 10 Hz), 4.38 (s, 3H), 3.36–3.34 (m, 2H), 3.23 (s, 3H), 3.04–3.01 (m, 1H); ^{13}C NMR (CDCl₃, 125 MHz): δ 168.6 (C=O), 158.1, 157.9, 148.4, 146.8, 135.3, 134.8, 133.2, 126.8, 125.5, 122.7, 120.7, 120.5, 119.5, 116.9, 114.0, 112.8, 36.2, 28.3 (CH₂), 15.8; HRMS (ESI) calcd. for C₁₉H₁₇N₃OS (M+H)⁺: 336.1176. Found: 336.1171.

2',3'-O-isopropylidene-5'-deoxy-5-fluoro-N⁴-[2-(tritylmercapto)acetyl]cytidine (**30**): Yield 73%; ^1H NMR (CDCl₃, 500 MHz): δ 7.59–7.59 (m, 1H, H-6), 7.58–7.20 (m, 15H, Ar-H), 5.64–5.63 (m, 1H, H-11), 5.30 (s, 1H, NH), 4.90–4.89 (m, 1H, H-12), 4.50–4.49 (m, 1H, H-13), 4.33–4.32 (m, 1H, H-14), 3.48 (brs, 2H, -CH₂-S-Tr), 1.57 (s, 3H, CH₃), 1.40 (d, 3H, H-15), 1.34 (s, 3H, CH₃); ^{13}C NMR (CDCl₃, 125 MHz): δ 171.1 (CO, -CO-CH₂-S-Tr), 152.3 (C-4), 143.9, 143.8, 129.4 (C-6), 129.3–128.0 (Ar-C), 114.5 (C-16), 94.3 (C-11), 85.3 (C-12), 84.8 (C-13), 83.8 (C-14), 38.8 (-CH₂-S-), 35.3, 34.1, 29.6, 29.3, 27.1 (C-18), 25.2 (C-17), 19.1 (C-15); HRMS (ESI) calcd. for C₃₃H₃₂O₅SFN₃ (M+Na)⁺: 624.1929. Found: 624.1944.

1-(5-deoxy- β -D-ribofuranosyl)-5-fluoro-1H-spiro[pyrimidine-4,2'-[1,3]thiazolidine]-2,4'-dione (**31**): The intermediate **30** (582 mg, 0.97 mM) was dissolved in 10 mL dichloromethane in argon atmosphere and cooled to 0 °C (ice bath). The colorless solution was treated with 2.0 mL of trifluoroacetic acid, and next, triethylsilane (0.5 mL) was immediately added to the reaction mixture. The reaction was monitored by TLC (hexane:ethyl acetate:methanol 5:3:1), and it was completed after 30 min. Then the reaction was quenched with triethylamine (1 mL), and solution was washed with water (20 mL) and brine (20 mL). The organic phase was evaporated to the oil at room temperature. The crude oil was dissolved in 6 mL methanol, and 1M HCl (3 mL) was added to the solution. The mixture was stirred for 20 min at room temperature. Next, water (10 mL) and ethyl acetate (20 mL) were added. The organic phase was separated, washed with brine, and dried over anhydrous MgSO₄. After evaporation, the oil was purified by column chromatography (hexane: ethyl acetate: methanol 5:3:1) to afford of **31** as a white solid (247 mg, 80%). m.p. 160.2 °C; ^1H NMR (CDCl₃, 500 MHz): δ 9.48 (brs, 1H, NH, H-7), 8.94–8.93 (m, 1H, NH, H-3), 6.76–6.74 (m, 1H, H-6), 5.57–5.56 (dd, 1H, H-11), 5.18–5.04 (m, 1H, OH), 5.00–4.94 (m, 1H, OH), 3.95–3.93 (m, 1H, H-12), 3.71–3.68 (m, 2H, H-14, -CH₂-S-), 3.61–3.57 (m, 2H, H-13, -CH₂-S-), 1.18 (s, 3H, CH₃); ^{13}C NMR (CDCl₃, 125 MHz): δ 170.0 (CO, -CO-CH₂-S), 148.5 (CO), 139.0 (d, *J* = 232.0 Hz, C-5), 110.2 (C-6), 87.9 (C-11), 78.4 (C-14), 77.2 (C-4), 74.2 (C-13), 71.2 (C-12), 33.8 (C-9), 18.9 (CH₃, C-15); HRMS (ESI) calcd. for C₁₁H₁₄O₅SFN₃ (M+Na)⁺: 342.0525. Found: 342.0536.

3.4. Theoretical Calculations

The density functional theory at the B3LYP/6-31G(d) level was used with the Gaussian G16 suite of programs [49]. The molecular geometries, harmonic frequencies, and the Gibbs free energies

were calculated following standard settings within the Gaussian code. For the largest molecule, **M25** (Figure 3, 115 atoms, 1135 basis functions), the numerical frequencies were used in order to overcome extreme demand of the available computer RAM memory for analytically calculated frequencies. In selected cases, the semiempirical quantum mechanical PM7 method [49, also available in 48] was used for preliminary studies of 3D structure of larger complexes.

4. Conclusions

In summary, we described here the synthesis of several various biologically active compounds modified with a thiol-linker. This simple two-step procedure provides an advantageous method for the synthesis of thiol analogues useful for potential building their conjugates with nanoparticles. Moreover, the above methodology has given access to new sulfur derivatives, which might have potential therapeutic benefits. Further studies, focusing on the building of conjugates of thiol-containing derivatives with gold nanoparticles, will be published elsewhere.

Supplementary Materials: The Supplementary Materials are available online. Figure S1: The initial step of the **22** deprotection when **22** is surrounded by the Et₃SiH and four TFA molecules; Figure S2: The initial step of the **24** deprotection when **24** is surrounded by the Et₃SiH and four; Figure S3: The hypothetical deprotection product of the **22** molecule surrounded by the Et₃SiOCCF₃, triphenyl methane and three TFA molecules; Figure S4: The deprotection product **26** of the **24** molecule surrounded by the Et₃SiOCCF₃, triphenyl methane and three TFA molecules; ¹H and ¹³C NMR spectra of compounds; The Cartesian coordinates, in Angstroms.

Author Contributions: K.S.: concept, design, performing the synthetic research, analyzing the data, and writing the manuscript. O.M.: performing the synthetic research, writing the part of manuscript. M.K.: performing the spectroscopy experiments. A.L.: performing the theoretical investigation, writing the part of manuscript. M.C.: writing the manuscript, contribution to the discussion of the synthetic results. E.U.S.: conceptualization, idea of thio-compounds in nanomedicines, J.D.: review and editing. All authors have read and agreed to the published version of the manuscript.

Funding: This work was supported under the framework of a statutory project of the Łukasiewicz Industrial Chemistry Institute (No 841333) funded by the Polish Ministry of Science and Higher Education. The calculations were performed at the Interdisciplinary Centre for Mathematical and Computational Modeling of the University of Warsaw (ICM UW, the computer grant G18-6) which is kindly acknowledged for allocating facilities and computer time. The authors are involved in the ORBIS project that received funding from the European Union's Horizon 2020 research and innovation program under the Marie Skłodowska-Curie grant agreement No 778051 and the Ministry of Science and Higher Education of Poland fund for supporting internationally co-financed projects in 2018–2022 (agreement No 3898/H2020/2018/2). The views expressed in this article are those of the authors and do not necessarily reflect the European Union's or the respective institution's position on the subject.

Conflicts of Interest: The authors declare no conflict of interest.

References

1. Feng, M.; Tang, B.; Liang, S.H.; Jiang, X. Sulfur containing scaffolds in drugs: Synthesis and application in medicinal chemistry. *Curr. Top. Med. Chem.* **2016**, *16*, 1200–1216. [[CrossRef](#)] [[PubMed](#)]
2. Lanterna, A.E.; Coronado, E.A.; Granados, A.M. When nanoparticle size and molecular geometry matter: Analyzing the degree of surface functionalization of gold nanoparticles with sulfur heterocyclic compounds. *J. Phys. Chem. C* **2012**, *116*, 6520–6529. [[CrossRef](#)]
3. Pensa, E.; Cortes, E.; Corthey, G.; Carro, P.; Vericat, C.; Fonticelli, M.H.; Benitez, G.; Rubert, A.A.; Salvarezza, R.C. The Chemistry of the sulfur gold interface: In search of a unified model. *Acc. Chem. Res.* **2012**, *45*, 1183–1192. [[CrossRef](#)] [[PubMed](#)]
4. Stolarczyk, E.U.; Sidoryk, K.; Cybulski, M.; Kubiszewski, M.; Stolarczyk, K. Design of therapeutic self-assembled monolayers of thiolated abiraterone. *Nanomaterials* **2018**, *8*, 1018. [[CrossRef](#)]
5. Tiwari, P.M.; Vig, K.; Dennis, V.A.; Singh, S.R. Functionalized gold nanoparticles and their biomedical applications. *Nanomaterials* **2011**, *1*, 31–63. [[CrossRef](#)]
6. Stolarczyk, E.U.; Leś, A.; Łaszcz, M.; Kubiszewski, M.; Strzempek, W.; Menaszek, E.; Fussaro, M.; Sidoryk, K.; Stolarczyk, K. The ligand exchange of citrates to thioabiraterone on gold nanoparticles for prostate cancer therapy. *Int. J. Pharm.* **2020**, *583*, 119319. [[CrossRef](#)]
7. Petros, R.A.; DeSimone, J.M. Strategies in the design of nanoparticles for therapeutic application. *Nat. Rev. Drug Discov.* **2010**, *9*, 615–627. [[CrossRef](#)]

8. Truong, L.; Zaikova, T.; Baldock, B.L.; Balik-Meisner, M.; Kimberly To, K.; Reif, D.M.; Kennedy, Z.C.; Hutchison, J.E.; Tangua, R.L. Systematic determination of the relationship between nanoparticle core diameter and toxicity for a series of structurally analogous gold nanoparticles in zebrafish. *Nanotoxicology* **2019**, *13*, 879–893. [[CrossRef](#)]
9. Javier, D.J.; Castellanos-Gonzalez, A.; Weigum, S.E.; Clinton White, A., Jr.; Richards-Kortum, R. Oligonucleotide-gold nanoparticle networks for detection of *Cryptosporidium parvum* Heat Shock Protein 70 mRNA. *J. Clin. Microbiol.* **2009**, *47*, 4060–4066. [[CrossRef](#)]
10. Li, X.; Li, H.; Yang, W.; Zhuang, J.; Li, H.; Wang, W. A mild and selective protecting and reversed modification of thiols. *Tetrahedron Lett.* **2016**, *57*, 2660–2663. [[CrossRef](#)]
11. Sidoryk, K.; Świtalska, M.; Jaromin, A.; Cmoch, P.; Bujak, I.; Kaczmarska, M.; Wietrzyk, J.; Dominguez, E.G.; Żarnowski, R.; Andes, D.R.; et al. The synthesis of indolo[2,3-b]quinoline derivatives with a guanidine group: Highly selective cytotoxic agents. *Eur. J. Med. Chem.* **2015**, *105*, 208–219. [[CrossRef](#)] [[PubMed](#)]
12. Sidoryk, K.; Świtalska, M.; Wietrzyk, J.; Jaromin, A.; Piętka-Ottlik, M.; Cmoch, P.; Zagrodzka, J.; Szczepek, W.J.; Kaczmarek, Ł.; Peczyńska-Czoch, W. Synthesis and biological evaluation of new amino acid and dipeptide derivatives of neocryptolepine as anticancer agents. *J. Med. Chem.* **2012**, *55*, 5077–5087. [[PubMed](#)]
13. Michalak, O.; Krzeczyński, P.; Cieślak, M.; Cmoch, P.; Cybulski, M.; Królewska-Golińska, K.; Kaźmierczak-Barańska, J.; Trzaskowski, B.; Ostrowska, K. Synthesis and anti-tumour, immunomodulating activity of diosgenin and tigogenin conjugates. *J. Steroid Biochem. Mol. Biol.* **2020**, *198*, 105573. [[CrossRef](#)] [[PubMed](#)]
14. Sidoryk, K.; Jaromin, A.; Edward, J.A.; Świtalska, M.; Stefańska, J.; Cmoch, P.; Zagrodzka, J.; Szczepek, W.; Peczyńska-Czoch, W.; Wietrzyk, J.; et al. Searching for new derivatives of neocryptolepine: Synthesis, antiproliferative, antimicrobial and antifungal activities. *Eur. J. Med. Chem.* **2014**, *78*, 304–313. [[CrossRef](#)] [[PubMed](#)]
15. Nascimento do, P.G.G.; Lemos, T.L.G.; Bizerra, A.M.C.; Arriaga, Â.M.C.; Ferreira, D.A.; Santiago, G.M.P.; Braz-Filho, R.; Galberto, M.; Costa, J. Antibacterial and antioxidant activities of ursolic acid derivatives. *Molecules* **2014**, *19*, 1317–1327. [[CrossRef](#)]
16. Saeidnia, S.; Manayi, A.; Gohari, A.R.; Abdollahi, M. The Story of Beta-sitosterol—A Review. *Eur. J. Med. Plants.* **2014**, *4*, 590–609. [[CrossRef](#)]
17. Panaretto, B.A.; Wallace, A.L.C. The administration of flumethasone, by three different routes, its measurement in the plasma and some effects on wool growth in merino wethers. *Aust. J. Biol. Sci.* **1978**, *31*, 601–619. [[CrossRef](#)]
18. Edin, H.M.; Andersen, L.B.; Schoaf, L.; Scott-Wilson, C.A.; Ho, S.Y.; Ortega, H.G. Effects of fluticasone propionate and salmeterol hydrofluoroalkane inhalation aerosol on asthma-related quality of life. *Ann. Allergy Asthma Immunol.* **2009**, *102*, 323–327. [[CrossRef](#)]
19. Cmoch, P.; Krzeczyński, P.; Leś, A. Multinuclear NMR measurements and DFT calculations for Capecitabine tautomeric form assignment in a solution. *Molecules* **2018**, *23*, 161. [[CrossRef](#)]
20. Walko, C.M.; Lindley, C. Capecitabine: A review. *Clin. Ther.* **2005**, *27*, 23–44. [[CrossRef](#)]
21. Gryniewicz, G.; Achmatowicz, O.; Pucko, W. Bioactive isoflavone—genistein; synthesis and prospective applications. *Herbal Pol.* **2000**, *46*, 151–160.
22. Tuli, H.S.; Tuorkey, M.J.; Thakral, F.; Sak, K.; Kumar, M.; Kumar Sharma, A.; Sharma, U.; Jain, A.; Aggarwal, V.; Bishayee, A. Molecular Mechanisms of Action of Genistein in Cancer: Recent Advances. *Front. Pharmacol.* **2019**, *10*, 1336. [[CrossRef](#)] [[PubMed](#)]
23. Tang, H.; Wang, S.; Li, X.; Zou, T.; Huang, X.; Zhang, W.; Chen, Y.; Yang, C.; Pan, Q.; Liu, H.-F. Prospects of and limitations to the clinical applications of genistein. *Discov. Med.* **2019**, *27*, 177–188. [[PubMed](#)]
24. Stolarczyk, E.U.; Stolarczyk, K.; Łaszcz, M.; Kubiszewski, M.; Maruszak, W.; Olejarz, W.; Bryk, D. Synthesis and characterization of genistein conjugated with gold nanoparticles and the study of their cytotoxic properties. *Eur. J. Pharm. Sci.* **2017**, *96*, 176–185. [[CrossRef](#)] [[PubMed](#)]
25. Stolarczyk, E.U.; Łaszcz, M.; Leś, A.; Kubiszewski, M.; Kuziak, K.; Sidoryk, K.; Stolarczyk, K. Design and Molecular Modeling of Abiraterone-Functionalized Gold Nanoparticles. *Nanomaterials* **2018**, *8*, 641. [[CrossRef](#)]
26. Stolarczyk, E.U.; Stolarczyk, K.; Łaszcz, M.; Kubiszewski, M.; Leś, A.; Michalak, O. Pemetrexed conjugated with gold nanoparticles—Synthesis, characterization and a study of noncovalent interactions. *Eur. J. Pharm. Sci.* **2017**, *109*, 13–20. [[CrossRef](#)]

27. Okawara, M.; Hashimoto, F.; Todo, H.; Sugibayashi, K.; Tokudome, Y. Effect of liquid crystals with cyclodextrin on the bioavailability of a poorly water-soluble compound, diosgenin, after its oral administration to rats. *Int. J. Pharm.* **2014**, *472*, 257–261. [[CrossRef](#)]
28. Baan, J.; MEM Bos, M.; U Gonesh-Kisoensingh, S.; Meynaar, I.A.; Alsmas, J.; Meijer, E.; GVulto, A. Capecitabine-induced Toxicity: An Outcome Study into Drug Safety. *J. Integr. Oncol.* **2014**, *3*. [[CrossRef](#)]
29. Du, Y.; Xia, L.; Jo, A.; Davis, R.M.; Bissel, P.; Ehrich, M.; Kingston, D.G.I. Synthesis and Evaluation of Doxorubicin-Loaded Gold Nanoparticles for Tumor-Targeted Drug Delivery. *Bioconjugate Chem.* **2018**, *29*, 420–430. [[CrossRef](#)]
30. Anwar, A.; Siddiqui, R.; Raza Shah, M.; Khan, N.A. Gold Nanoparticles Conjugation Enhances Antiacanthamoebic Properties of Nystatin, Fluconazole and Amphotericin B. *J. Microbiol. Biotechnol.* **2019**, *29*, 171–177. [[CrossRef](#)]
31. Singh, M.; Hamid, A.A.; Maurya, A.K.; Prakash, O.; Khan, F.; Kumar, A.; Aiyelaagbe, O.O.; Negi, A.S.; Bawankule, D.U. Synthesis of diosgenin analogues as potential anti-inflammatory agents. *J. Steroid Biochem. Mol. Biol.* **2014**, *143*, 323–333. [[CrossRef](#)] [[PubMed](#)]
32. Huang, B.Z.; Xin, G.; Ma, L.M.; Wei, Z.L.; Shen, Y.; Zhang, R.; Zheng, H.J.; Zhang, X.H.; Niu, H.; Huang, W. Synthesis, characterization, and biological studies of diosgenin analogs. *J. Asian Nat. Prod. Res.* **2017**, *19*, 272–298. [[CrossRef](#)] [[PubMed](#)]
33. Wakasugi, K.; Nakamura, A.; Tanabe, Y. Me₂NSO₂Cl and N,N-dimethylamines; a novel and efficient agent for esterification, amidation between carboxylic acids, and equimolar amounts of alcohols and amines. *Tetrahedron Lett.* **2001**, *42*, 7427–7430. [[CrossRef](#)]
34. Kawabata, T.; Mizugaki, T.; Ebitani, K.; Kaneda, K. Highly efficient esterification of carboxylic acids with alcohols by montmorillonite-enwrapped titanium as a heterogeneous acid catalyst. *Tetrahedron Lett.* **2003**, *44*, 9205–9208. [[CrossRef](#)]
35. Lee, S.G.; Park, J.H. Metallic Lewis acids-catalyzed acetylation of alcohols with acetic anhydride and acetic acid in ionic liquids: Study on reactivity and reusability of the catalysts. *J. Mol. Catal. A Chem.* **2003**, *194*, 49–52. [[CrossRef](#)]
36. Chen, C.T.; Munot, Y.S. Direct Atom-Efficient Esterification between Carboxylic Acids and Alcohols Catalyzed by Amphoteric, Water-Tolerant TiO(acac)₂. *J. Org. Chem.* **2005**, *70*, 8625–8627. [[CrossRef](#)]
37. Ishihara, K.; Nakagawa, S.; Sakakura, A. Bulky Diarylammonium Arenesulfonates as Selective Esterification Catalysts. *J. Am. Chem. Soc.* **2005**, *127*, 4168–4169. [[CrossRef](#)]
38. Khalafi-Nezhad, A.; Parhami, A.; Zare, A.; Moosavi Zare, A.R. Efficient method for the direct preparation of aryl carboxylates from carboxylic acids using tosyl chloride under solvent-free conditions. *J. Iran. Chem. Soc.* **2008**, *5*, 413–419. [[CrossRef](#)]
39. Gilles, V.; Vieira, M.A.; Lacerda, V., Jr.; Castro, E.V.R.; Santos, R.B.; Orestes, E.; Carneiro, J.W.M.; Greco, S.J. A new, simple and efficient method of steglich esterification of Juglone with long-fatty acids: Synthesis of a new class of non-polymeric wax deposition inhibitors for crude oil. *J. Braz. Chem. Soc.* **2015**, *26*, 74–83. [[CrossRef](#)]
40. Drouet, S.; Doussot, J.; Garros, L.; Mathiron, D.; Bassard, S.; Favre-Reguillon, A.; Molinier, R.; Laine, E.; Hano, C. Selective synthesis of 3-O-palmitoyl-sylibyn, a new-to-nature flavonolignan with increased protective action against oxidative damages in lipophilic media. *Molecules* **2018**, *23*, 2594. [[CrossRef](#)]
41. Kicsak, M.; Bege, M.; Bereczki, I.; Csavas, M.; Herczeg, M.; Kupihar, Z.; Kovacs, L.; Borbas, A.; Herczegh, P. A tree-component reagent system for rapid and mild removal of O-, N-, S-trityl protecting groups. *Org. Biomol. Chem.* **2016**, *14*, 3190–3192. [[CrossRef](#)] [[PubMed](#)]
42. Gryniewicz, G.; Zegrocka-Stendel, O.; Pucko, W.; Ramza, J.; Kościelecka, A.; Kołodziejki, W.; Woźniak, K. X-ray and ¹³C CP MAS investigation of structure of two genistein derivatives. *J. Mol. Struct.* **2004**, *694*, 121–129. [[CrossRef](#)]
43. Szeja, W.; Puchałka, J.; Świerk, P.; Hendrich, A.B.; Gryniewicz, G. Selective alkylation of genistein and daidzein. *Chem. Biol. Interface* **2013**, *3*, 95–106.
44. Ingle, G.K.; Mormino, M.G.; Wojtas, L.; Antilla, J.C. Chiral phosphoric acid-catalyzed addition of thiol to N-acyl imines: Access to chiral N,S-acetals. *Org. Lett.* **2011**, *13*, 4822–4825. [[CrossRef](#)]
45. Nakamura, S.; Takahashi, S.; Nakane, D.; Masuda, H. Organocatalytic enantioselective addition of thiols to ketimines derived from isatins. *Org. Lett.* **2015**, *2*, 106–109. [[CrossRef](#)]
46. Wang, H.Y.; Zhang, J.X.; Cao, D.D.; Zhao, G. Enantioselective addition of thiols to imines catalysed by thiourea-quaternary ammonium salts. *ACS Catal.* **2013**, *3*, 2218–2221. [[CrossRef](#)]

47. Imagawa, H.; Tsuchihashi, T.; Singh, R.K.; Yamamoto, H.; Sugihara, T.; Nishizawa, M. Triethyl-(or trimethyl-)silyl triflate-catalyzed reductive cleavage of triphenylmethyl (trityl) ethers with triethylsilane. *Org. Lett.* **2003**, *5*, 153–155. [[CrossRef](#)]
48. Frisch, M.J.; Trucks, G.W.; Schlegel, H.B.; Scuseria, G.E.; Robb, M.A.; Cheeseman, J.R.; Scalmani, G.; Barone, V.; Petersson, G.A.; Nakatsuji, H.; et al. *Gaussian 16, Revision A.03*; Gaussian, Inc.: Wallingford CT, UK, 2016.
49. *MOPAC2016*, J.J.P.; Stewart, Stewart Computational Chemistry: Colorado Springs, CO, USA, 2016.

Sample Availability: Samples of the compounds are not available from the authors.



© 2020 by the authors. Licensee MDPI, Basel, Switzerland. This article is an open access article distributed under the terms and conditions of the Creative Commons Attribution (CC BY) license (<http://creativecommons.org/licenses/by/4.0/>).